Graff's Textbook of Urinalysis and Body Fluids

THIRD EDITION

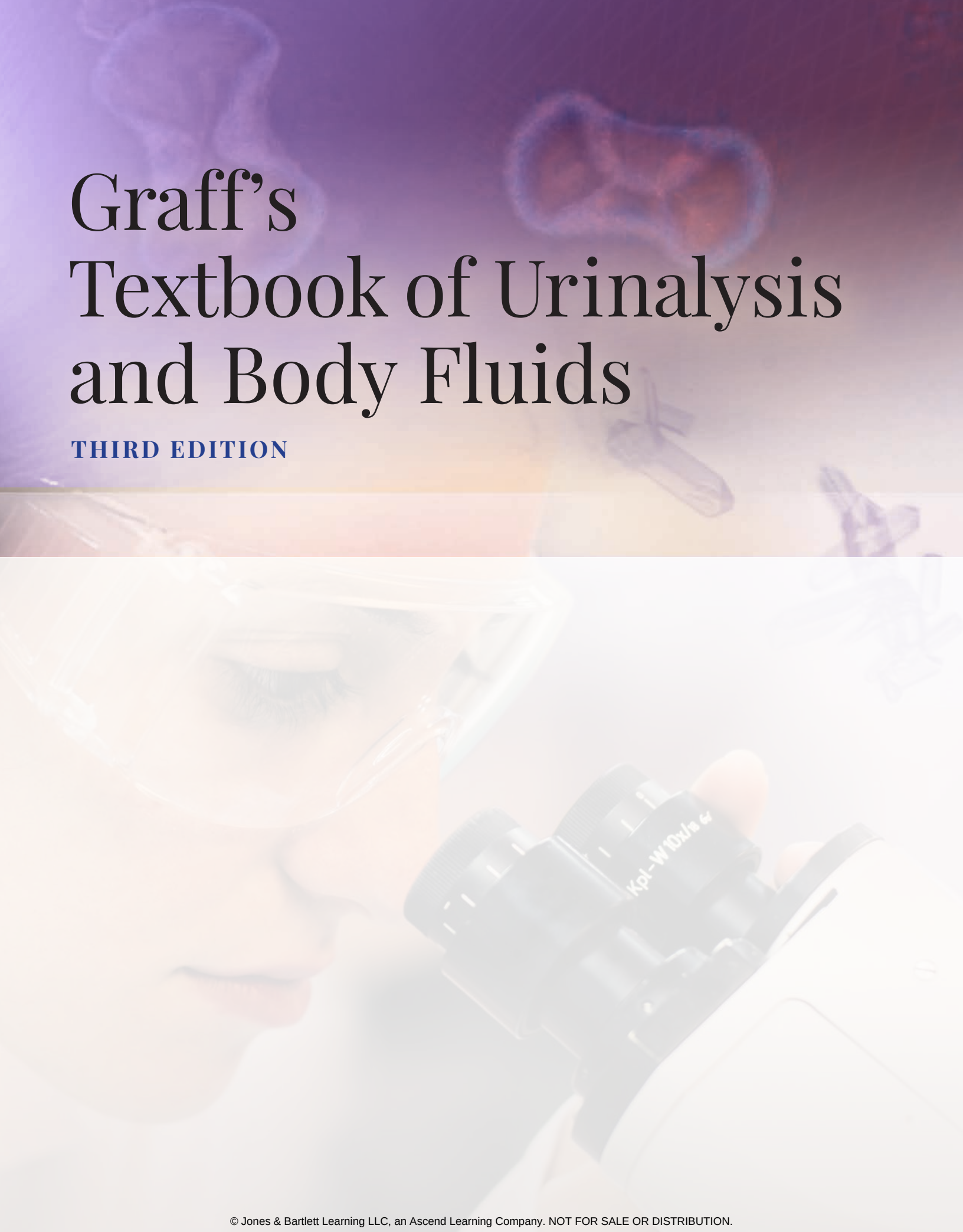

© Jones & Bartlett Learning LLC, an Ascend Learning Company. NOT FOR SALE OR DISTRIBUTION.

© Jones & Bartlett Learning LLC, an Ascend Learning Company. NOT FOR SALE OR DISTRIBUTION.

Graff's Textbook of Urinalysis and Body Fluids

THIRD EDITION

Lillian A. Mundt, EdD, MLS(ASCP)SH
Adventist Health Systems
Hinsdale Hospital, Hinsdale, IL
LaGrange Memorial Hospital, LaGrange, IL

Kristy Shanahan, MS, MLS(ASCP)
Assistant Professor
Rosalind Franklin University of Medicine and Science
North Chicago, IL

JONES & BARTLETT
LEARNING

© Jones & Bartlett Learning LLC, an Ascend Learning Company. NOT FOR SALE OR DISTRIBUTION.

World Headquarters
Jones & Bartlett Learning
5 Wall Street
Burlington, MA 01803
978-443-5000
info@jblearning.com
www.jblearning.com

Jones & Bartlett Learning books and products are available through most bookstores and online booksellers. To contact Jones & Bartlett Learning directly, call 800-832-0034, fax 978-443-8000, or visit our website, www.jblearning.com.

Substantial discounts on bulk quantities of Jones & Bartlett Learning publications are available to corporations, professional associations, and other qualified organizations. For details and specific discount information, contact the special sales department at Jones & Bartlett Learning via the above contact information or send an email to specialsales@jblearning.com.

Copyright © 2016 by Jones & Bartlett Learning, LLC, an Ascend Learning Company

All rights reserved. No part of the material protected by this copyright may be reproduced or utilized in any form, electronic or mechanical, including photocopying, recording, or by any information storage and retrieval system, without written permission from the copyright owner.

The content, statements, views, and opinions herein are the sole expression of the respective authors and not that of Jones & Bartlett Learning, LLC. Reference herein to any specific commercial product, process, or service by trade name, trademark, manufacturer, or otherwise does not constitute or imply its endorsement or recommendation by Jones & Bartlett Learning, LLC and such reference shall not be used for advertising or product endorsement purposes. All trademarks displayed are the trademarks of the parties noted herein. *Graff's Textbook of Urinalysis and Body Fluids, Third Edition* is an independent publication and has not been authorized, sponsored, or otherwise approved by the owners of the trademarks or service marks referenced in this product.

There may be images in this book that feature models; these models do not necessarily endorse, represent, or participate in the activities represented in the images. Any screenshots in this product are for educational and instructive purposes only. Any individuals and scenarios featured in the case studies throughout this product may be real or fictitious but are used for instructional purposes only.

This publication is designed to provide accurate and authoritative information in regard to the Subject Matter covered. It is sold with the understanding that the publisher is not engaged in rendering legal, accounting, or other professional service. If legal advice or other expert assistance is required, the service of a competent professional person should be sought.

22140-4

Production Credits
VP, Product Management: Amanda Martin
Director of Product Management: Cathy Esperti
Product Manager: Sean Fabery
Product Specialist: Andrew LaBelle
Product Coordinator: Elena Sorrentino
Digital Project Specialist: Angela Dooley
Director of Marketing: Andrea DeFronzo
Marketing Manager: Dani Burford
Production Services Manager: Colleen Lamy
VP, Manufacturing and Inventory Control: Therese Connell
Composition: S4Carlisle Publishing Services
Project Management: S4Carlisle Publishing Services
Cover Design: Kristin E. Parker
Rights Specialist: Rebecca Damon
Printing and Binding: LSC Communications

Library of Congress Cataloging-in-Publication Data
Library of Congress Cataloging-in-Publication Data unavailable at time of printing.

LCCN: 2020937810

6048

Printed in the United States of America

24 23 22 21 20 10 9 8 7 6 5 4 3 2 1

© Jones & Bartlett Learning LLC, an Ascend Learning Company. NOT FOR SALE OR DISTRIBUTION.

We dedicate this book to our families who were patient and encouraged us while we spent valuable time away from them working on this project.

We also dedicate this book to medical laboratory students, instructors, and practitioners to whom this text and its ancillaries will prove to be a valuable resource.

© Jones & Bartlett Learning LLC, an Ascend Learning Company. NOT FOR SALE OR DISTRIBUTION.

© Jones & Bartlett Learning LLC, an Ascend Learning Company. NOT FOR SALE OR DISTRIBUTION.

Contributor

Jeanne M. Isabel EdD, MLS, SH
Northern Illinois University
College of Health and Human Sciences
DeKalb, Illinois

Reviewers

The authors would like to thank the following for reviewing current and previous editions.

Kay Hanna
Stark State College of Technology
North Canton, Ohio

Liz Johnson
Apollo College
Albuquerque, New Mexico

Julie Hammerling
Florida Gulf Coast University
Fort Myers, Florida

Danyel Anderson
Ozarks Technical Community College
Springfield, Missouri

Janice Miller
Northcentral Technical College
Wausau, Wisconsin

Sherry Parsons
Wichita Area Technical College
Wichita, Kansas

Sondra Sutherland
Jefferson Community College
Steubenville, Ohio

Jeanne M. Isabel
Northern Illinois University
DeKalb, IL

© Jones & Bartlett Learning LLC, an Ascend Learning Company. NOT FOR SALE OR DISTRIBUTION.

© Jones & Bartlett Learning LLC, an Ascend Learning Company. NOT FOR SALE OR DISTRIBUTION.

Preface

Sister Graff's *A Handbook of Routine Urinalysis* had served the clinical laboratory profession as a classic reference text of urine testing and atlas of urinary sediment from 1983 to 2011, when it was revised for the second edition to add chapters on body fluid analysis. Our goal for the third edition of this text is continually to preserve the integrity and importance of Sister Graff's work while expanding its use as a valuable resource for students, instructors, and laboratory professionals.

The second edition had substantially revised and enhanced the content to bring it up-to-date and expanded the text by including other body fluids, Chapter Objectives, Key Terms, Terms, Study Questions, Case Studies, and a Glossary to make the text more user friendly in the classroom. These updates and additions were reflected in the new title, *Graff's Textbook of Urinalysis and Body Fluids.*

This, the third edition continues to provide students, instructors, and laboratory professionals with updated information concerning urine and body fluid analyses. The expanded urinalysis and body fluids coverage in this text is comprehensive, clearly presented, and explained in easy-to-understand language. Continuing the standard set by Sister Graff, the book uses numerous color photomicrographs to familiarize readers with both the normal and abnormal structures found in the urinary sediment and body fluids while tables and illustrations help clarify concepts. The third edition is divided into three sections for better grouping of content.

Section I includes foundational information about renal anatomy (Chapter1) and disorders that may be detected by analyzing urine (Chapters 2 and 3), as well as introductory information regarding clinical laboratory operations including safety (Chapter 4) and microscopy (Chapter 5).

Section II focusses on the urinalysis, beginning with urine specimen collection and preservation (Chapter 6), then progressing through physical examination (Chapter 7), chemical analysis (Chapter 8), and microscopic examination including 17 new images (Chapter 9), ending with the central chapter and jewel of *Graff's Textbook of Urinalysis and Body Fluids,* the atlas of urinary sediment containing (Chapter 10). Instructors, students, and clinicians will find that no other text includes a comparable atlas.

Section III contains revised information as well as new information about various body fluid analyses beginning with an introduction (Chapter 11) and goes into further depth about: cerebrospinal fluid (Chapter 12), serous body fluids (Chapter 13), synovial fluid (Chapter 14), gastric fluid and fecal analysis (Chapter 15), semen analysis (Chapter 16), amniotic fluid (Chapter 17), vaginal secretions (Chapter 18), and miscellaneous body fluids (Chapter 19). Several new images have been added to this section to provide for better comprehension of the information presented.

The book wraps up with a chapter on automated methods and equipment (Chapter 20); Appendices provide answers to the study and case questions, historically relevant urinalysis information, reagent strip color chart, and a detailed explanation of manual hemocytometer cell count. A glossary of terms that is ideal for study and review summaries key terms highlighted in chapter; and for those who rely on the text as a reference, a complete index.

We note that the information concerning reactions of the various reagent strip methods is up-to-date at the time of publication, but because manufacturers continually improve their products, the reagents, sensitivities, detection ranges, and timings may change. Therefore, following manufacturers' most recent directions is of utmost importance.

We are grateful for the thoughtful suggestions of our reviewers and readers, to which we have given consideration when revising and updating the current text to meet the needs of our audience.

Graff's Textbook of Urinalysis Body Fluids will continue to serve the medical laboratory profession

© Jones & Bartlett Learning LLC, an Ascend Learning Company. NOT FOR SALE OR DISTRIBUTION.

© Jones & Bartlett Learning LLC, an Ascend Learning Company. NOT FOR SALE OR DISTRIBUTION.

Content Highlights

SECTION I FOUNDATIONAL INFORMATION

- **Chapter 1,** ***Urinary System Anatomy and Physiology and Urine Formation,*** contains the basic information on anatomy and physiology that is key to understanding the urinary system and urinalysis. While retaining the previous anatomy sections and the 17 related illustrations, the revised chapter has more information on urinary tract functions and on assessing renal function than the previous edition. The chapter has added information on creatinine clearance and calculating and estimating the glomerular filtration rate and using that information to assess chronic kidney disease stages. It also has included information on additional testing to assess renal function and basic information on assessing tubular reabsorption and secretion.
- **Chapter 2,** ***Renal and Urinary Tract Diseases and Related Urinalysis Findings***, has been split from the metabolic diseases that were together in Chapter 7 of the previous edition. This chapter includes expanded and updated information on acute kidney injury (AKI), which is a common problem in hospitalized patients, and recognizing the AKI stages. AKI has poor prognosis with a high associated mortality in hospitalized patients, particularly in the intensive care unit. This chapter also has expanded information and images on urolithiasis, which is a relative common and frequently recurring malady that occurs in the urinary tract. This is often a painful condition that has been found to have comorbidities with other conditions that affect the urinary tract.
- **Chapter 3,** ***Metabolic Diseases and Related Urinalysis Findings*** has been split from the renal diseases that were together in Chapter 7 of the previous edition. This chapter provides an overview of the most common metabolic diseases that are detectable with urine testing such as aminoacidurias, and carbohydrate metabolism disorders. A table explaining urine findings in porphyria, metabolic pathways, and five new images enhance the reader's understanding.
- **Chapter 4,** ***Urinalysis Clinical Laboratory Operations*** (Chapter 1 in the second edition) provides an overview of various regulatory agencies that have an influence laboratory operations and explains levels of testing as categorized in CLIA'88. The fundamentals of quality assessment are also covered as are principles for safe practices in the medical laboratory including an explanation of the Globally Harmonized System for labeling chemicals. Five new images have been added to this chapter, for a total of seven.
- **Chapter 5,** ***Microscopy*** is a new chapter for this edition drawing from the work of Landy McBride. This chapter includes the basics of microscope handling along with principles of illumination and how to achieve the best contrast for proper viewing. Several types of microscopy are presented. This chapter contains 25 images new to this text.

SECTION II THE URINALYSIS

- **Chapter 6** pulls out the **Collection and Preservation of Urine** information that was contained in Chapter 3 of the second edition, Collection and Physical Examination of Urine, into its own chapter. The previous edition only included one image for the collection and preservation information. The third edition contains seven additional images, including illustration of suprapubic puncture for the collection on urine directly from the bladder, collection containers, methods of transfer from collection container to urine testing tubes, and an assortment of urine preservative tubes. This chapter now contains eight images (seven new plus one reused as a chapter review question).
- **Chapter 7** pulls out the **Physical Examination of Urine** information that was contained in Chapter 3 of the second edition, Collection and Physical Examination of Urine, into its own chapter. The third edition contains images of abnormal urines, and an example of a "flow-through" set up for refractometry. This chapter now contains eight images (four new plus one reused as a chapter review question).
- **Chapter 8, Chemical Examination of Urine,** the third edition contains tables, chemical reactions, and images from the previous edition and clarifies procedures by enclosing this information in "boxes." In addition, urine reagent strip tests for ascorbate, calcium, creatinine, and microalbumin are included along with new images. This chapter now contains 23 images (12 new).
- **Chapter 9,** ***Microscopic Examination of Urinary Sediment*** continues to detail the observance of urinary sediment and includes 17 new images, some of rarely seen sediment. This chapter now contains 97 images.
- **Chapter 10,** ***Atlas of Urinary Sediment*** continues to be one of the most complete resources for urinary sediment

© Jones & Bartlett Learning LLC, an Ascend Learning Company. NOT FOR SALE OR DISTRIBUTION.

images. Most of the 190 images have been resized, while three have been replaced.

SECTION III BODY FLUIDS ANALYSIS

- **Chapter 11, *Introduction to Body Fluids***, along with its six images, is a basic overview of the types of fluids in the body, the formation of effusions and the methods for enumerating cells in these fluids.
- **Chapter 12, *Cerebrospinal Fluid*** contains a brief overview of the anatomy and physiology of CSF. Laboratory testing is detailed, and conditions affecting CSF test results are outlined. Eight new images have been added to this chapter for a total of 29.
- **Chapter 13, *Serous Body Fluids*** contains information about laboratory analysis of pleural, pericardial, and peritoneal fluids. Five new images have been added to this chapter for a total of 22.
- **Chapter 14, *Synovial Fluid*** contains a brief overview of the composition and function of synovial fluid. Laboratory analysis of synovial fluid is explained along with interpretation. This chapter contains 22 images.
- **Chapter 15, *Gastric Fluid and Fecal Analysis*** has been expanded to include gastric fluid information, which was not included in the second edition. An image of gastric fluid collection is included as well as an image for the testing of gastric fluid. An image has been added to the physiology section at the beginning of the chapter to provide students with an overview or review of the digestive system; and an additional image is added to the fecal analysis section. This chapter contains nine images (three new).
- **Chapter 16, *Semen Analysis*** provides information about the composition of semen and sperm formation, classification of semen by using various test parameters, and macroscopic and microscopic evaluation of semen. This chapter contains 27 images.
- **Chapter 17, *Amniotic Fluid*** contains information moved from the chapter on miscellaneous body fluids in the second edition into its own chapter. Three of this chapter's six images are new to this edition.
- **Chapter 18, *Vaginal Secretions*** contains information moved from the chapter on miscellaneous body fluids in the second edition into its own chapter and now covers the detection of fetal substances in vaginal secretions at the time of fetal membrane rupture prior to delivery. Six of this chapter's ten mages are new to this edition.
- **Chapter 19, *Miscellaneous Body Fluids***, is the most revised of all the chapters in the third edition. Sections from the second edition Chapter 14, Miscellaneous Body Fluids, that were removed and made into their own chapters include Amniotic Fluid and Vaginal Secretions. The information remaining from the previous Chapter 14, Urine Pregnancy Testing, and Bronchoalveolar Lavage and Bronchial Washings, is found in this chapter and includes six new images including an illustration to help students visualize the collection of bronchial fluid. New information not contained in the second edition, includes sections on Urine Eosinophils, Ear Fluidand Vitreous Fluid, along with three new images. The chapter now contains 18 images (10 new).
- **Chapter 20, *Automation of Urinalysis and Body Fluid Examination***, presents up-to-date information and images from several manufacturers of instrumentation for the analysis of urine and body fluids, including semen. In addition, 11 new images, screen shots from automated microscopic analysis of urine, are included for common urinary sediments. This chapter includes 32 images.

APPENDICES

- **Appendix A, *Answers to Study Guide Questions and Case Studies***, allows students to verify their comprehension of the material presented in the end of chapter questions.
- **Appendix B, *Reagent Strip Color Chart***, gives students to opportunity to view the color chart for manual interpretation of urine chemistry analysis prior to hands on laboratory sessions.
- **Appendix C, *Hemocytometer Cell Counts***, details manual cells counting principles. Seven new images are included to enhance understanding.
- **Appendix D, *Historically Relevant Urinalysis Information***, preserves methods used in the past as it provides for an understanding of the evolution of current methods. In addition, this appendix includes procedures that may still be performed by some laboratories.
- **Glossary,** now contains over 180 additional words. Watch for crossword puzzles to be made available on the Navigate 2 Companion Website.

ANCILLARY MATERIALS

Ancillary materials for users of *Graff's Textbook of Urinalysis and Body Fluid 3e* are available through the Navigate 2 Companion Website.

- PowerPoint Presentations
- Flashcards
- Crossword Puzzles
- Additional Case Studies

© Jones & Bartlett Learning LLC, an Ascend Learning Company. NOT FOR SALE OR DISTRIBUTION.

About the Authors

Lillian A. Mundt, EdD, MLS(ASCP)SH, LMT (NCBMT) is a medical laboratory scientist, massage therapist, curriculum designer, and author. Her background includes a bachelor's degree in medical technology, a master's degree in health professions education, and a doctorate in educational leadership. For over 30 years, she has developed and taught phlebotomy programs, clinical laboratory science programs, and graduate programs at both hospital-based and university-based institutions. She has authored and developed course materials used in online education programs for colleges and universities, as well as online continuing education companies. In addition, Dr. Mundt has authored several articles for professional journals, and has co-authored books on urinalysis, phlebotomy, a book chapter in clinical chemistry, and has published her dissertation. Dr. Mundt has presented posters and lectures at local, state, and national conventions. Her current focus is on developing educational materials for medical laboratory science and health professions education. She remains professionally current maintaining licensure as a massage therapist, employment as a medical laboratory scientist at a hospital laboratory, and developing and teaching courses on a contractual basis.

Kristy L. Shanahan, MS, MLS(ASCP)^{CM}, is a medical laboratory scientist, assistant professor in the Pharmaceutical Sciences department, biochemistry graduate student, and author. Her background includes a master's degree in clinical laboratory science, as well as a master's degree in biotechnology. She has many years of experience working in hospital and microbiology laboratories and has taught in biology, microbiology, and in medical laboratory technician and medical laboratory science programs from the associate degree level to the graduate level. She is currently teaching full-time in the College of Pharmacy at Rosalind Franklin University. She has developed course materials and taught in online courses for several community colleges and universities. Assistant Professor Shanahan has published articles in multiple journals, and has co-authored a book on urinalysis and a book chapter in clinical chemistry. She has presented posters and lectures at local, state, and national for medical laboratory science and microbiology professional programs. She is an active member of several professional groups in medical laboratory sciences, microbiology, and pharmacy.

© Jones & Bartlett Learning LLC, an Ascend Learning Company. NOT FOR SALE OR DISTRIBUTION.

© Jones & Bartlett Learning LLC, an Ascend Learning Company. NOT FOR SALE OR DISTRIBUTION.

Acknowledgments

Thank you to Landy James McBride PhD, MT(ASCP), Professor Emeritus of Biology (1983–2002) California State University, Bakersfield, CA for content and images that comprise most of Chapter 5: Microscopy.

We thank our reviewers for their insightful suggestions for improving the third edition of this text. We greatly appreciate the expertise, cooperation, and patience of the publisher and editing managers who assisted us.

In addition, we thank the various manufacturers for images of their instruments.

Finally, we thank the Pathology Laboratory at Adventist Hinsdale Hospital and Adventist LaGrange Memorial Hospital, IL, for supplying specimens from which new images were created; and co-worker for her modeling of laboratory procedures.

© Jones & Bartlett Learning LLC, an Ascend Learning Company. NOT FOR SALE OR DISTRIBUTION.

© Jones & Bartlett Learning LLC, an Ascend Learning Company. NOT FOR SALE OR DISTRIBUTION.

List of Figures

1-1. Male urinary tract—lateral view. (Adapted with permission from Anatomical Chart Company, Inc., Skokie, IL, USA.) 3

1-2. Female urinary tract—lateral view. (Adapted by permission from Anatomical Chart Company, Inc., Skokie, IL, USA.) 3

1-3. The urinary system. (Asset provided by Anatomical Chart Co.) 4

1-4. Structures of the urinary tract **(A)**, and cross-section of the kidney **(B).** 5

1-5. The kidney. 5

1-6. The sectioned left kidney. 6

1-7. The nephron. (Asset provided by Anatomical Chart Co.) 7

1-8. In this view the nephron has been stretched out and the surrounding blood vessels removed to illustrate the different sections of the tubule. The reabsorption of sodium and water is indicated. (From Cohen BJ, Taylor JJ. (2005). *Memmler's The Human Body in Health and Disease*, 10th ed. Burlington, MA: Jones & Bartlett Learning, LLC.) 8

1-9. Renal arterial and venous blood flow through the kidney. 8

1-10. The renal pyramid with corresponding blood vessels. (Asset provided by Anatomical Chart Co.) 9

1-11. Bowman capsule, the glomerular tuft, and the juxtaglomerular apparatus. (From Gartner H. *Color Atlas of Histology*, 3rd ed. Philadelphia, PA: Lippincott Williams & Wilkins, 2001.) 9

1-12. The glomerulus (renal corpuscle) and the filtration barrier of the glomerulus. (Asset provided by Anatomical Chart Co.) 9

1-13. Formation of urine via filtration, reabsorption, secretion, and hormonal effects. (From Premkumar K. *The Massage Connection Anatomy and Physiology*. Baltimore, MA: Lippincott Williams & Wilkins, 2004.) 10

1-14. Filtration and tubular processing of the glomerular ultrafiltrate. 10

1-15. The countercurrent mechanism and antidiuretic hormone in urine concentration. (From Premkumar K. *The Massage Connection Anatomy and Physiology*. Baltimore, MA: Lippincott Williams & Wilkins, 2004.) 11

1-16. The renin–angiotensin–aldosterone cycle and hypertension. (Asset provided by Anatomical Chart Co.) 12

1-17. Renal cell becoming an oval fat body. Note the Maltese-cross formations inside the cell, indicating the lipid droplets contained in this cell. Eventually, the cell will become unrecognizable as a cell as it takes on more lipids, and it will become an oval fat body. 13

2-1. Comparison of different types of kidney stones: Clinical manifestations of kidney stones include hematuria and flank pain. 20

2-2. Magnesium ammonium Phosphate (Struvite) Stones in Kidney Labeled Asset provided by Anatomical Chart Co. 21

2-3. Hydronephrosis and Kidney Stone Labeled Asset provided by Anatomical Chart Co. 21

2-4. Vesicle Kidney Stones Labeled. 21

2-5. Glomerulus with single well-developed Kimmelstiel–Wilson nodule at 12 o'clock. Also note uniform thickening of GBM. (PAS, ×390.) 30

2-6. RBC cast: urine sediment; 400×. (University of Washington Department of Laboratory Medicine, with permission.) 31

2-7. Broad finely granular cast becoming waxy cast with mixed cellular background. (Courtesy of McBride LJ. *Textbook of Urinalysis and Body Fluids: A Clinical Approach.* Philadelphia, PA: Lippincott, 1998.) 31

2-8. Fatty casts, urine sediment; 400×. (University of Washington Department of Laboratory Medicine, with permission.) 32

2-9. Fatty casts; polarized light (POL); urine sediment; 400×. (University of Washington Department of Laboratory Medicine, with permission.) 32

2-10. Granular casts, urine sediment. SM stain; 200×. (Courtesy of McBride LJ. *Textbook of Urinalysis and Body Fluids: A Clinical Approach.* Philadelphia, PA: Lippincott, 1998.) 32

2-11. WBC cast, urine sediment. SM stain; 400×. (Courtesy of McBride LJ. *Textbook of Urinalysis and Body Fluids: A Clinical Approach.* Philadelphia, PA: Lippincott, 1998.) 32

2-12. Direct Gram stain of urine showing gram-negative rod bacteria and three WBCs (neutrophils); 1000×. (Courtesy of McBride LJ. *Textbook of Urinalysis and Body Fluids: A Clinical Approach.* Philadelphia, PA: Lippincott, 1998.) 33

3-1. **A:** Diaper with urine from normal infant. **B:** Diaper with urine from infant with Hartnup syndrome.

3-2. The normal metabolic pathway of phenylalanine metabolism. 36

3-3. Increased formation of phenylalanine metabolites resulting from the deficiency of phenylalanine hydroxylase. 36

3-4. Types of tyrosinemia depend on the enzyme that is deficient. 37

3-5. Tyrosine also has another metabolic pathway, the production of melanin. Albinism results from a deficiency in tyrosinase. 37

3-6. Alkaptonuria results from a deficiency in homogentisic acid oxidase. 38

3-7. Biosynthesis of heme. (Porphyrins are underlined). 39

3-8. Urine containing porphyrins under ultraviolet light. 40

3-10. Diaper with urine from infant with Lesch–Nyhan disease. Note the "red brick dust" appearance of the urine acid crystal clumps. 40

3-11. Image for Case study 3-1. 42

3-12. Image for Case study 3-3. 43

© Jones & Bartlett Learning LLC, an Ascend Learning Company. NOT FOR SALE OR DISTRIBUTION.

4-1. Common safety symbols. (Courtesy of McBride L. *Textbook of Urinalysis and Body Fluids*. Philadelphia, PA: Lippincott; 1998.) 49

4-2. Global Harmonization System pictograms used for chemical hazard communication (as found on the OSHA web site). 50

4-3. National Fire Protection Agency (NFPA) symbol. 50

4-4. Hazardous Materials Identification System (HMIS) label. 50

4-5. A table-top safety shield is one engineering device that can be used to protect personnel when handling specimens or chemicals. 51

4-6. A chemical spill cleanup kit contains the materials needed to clean up various types of chemical spills. 51

4-7. Sinks designated as **(A)** "clean" for hand washing and **(B)** "dirty" for processing of specimens should be clearly marked and their uses enforced. 52

5-1. Ray diagram of a simple microscope. The object is imaged on the retina of the eye by the lens. This appears to the eye as if it were from an object at the position of the virtual image. (From Richardson H. *Handbook for the light microscope: A user's guide*. Park Ridge, NJ: Noyes Publications; 1991.) 56

5-2. Ray diagram of a compound microscope; the object is just outside of the first focal plane of the objective (FOB); the intermediary image is just within the focal plane of the eyepiece FOC; compare with 8-1. (From James J. *Light Microscope Techniques in Biology and Medicine*. Dordrecht: Kluwer Academic Publishers; 1976.) 56

5-3. Schematic relationship between the virtual image as perceived by the eye and the real image that exists above the eyepiece; this latter image is the one used for photomicrography. (From Richardson H. *Handbook for the light microscope: A user's guide*. Park Ridge, NJ: Noyes Publications; 1991.) 56

5-4. Ray diagram of a compound microscope. (From James J, Tanke HJ, eds. *Biomedical Light Microscopy*. Dordrecht: Kluwer Academic Publishers; 1976.) 57

5-5. Spherical aberration. When the object is a luminous point emitting monochromatic light, a bright circle with darker border will be seen on a screen held in the object space at A; at plane B a bright ring with a darker center will be seen. AP-angular aperture of the lens. (From James J. *Light Microscope Techniques in Biology and Medicine*. Dordrecht: Kluwer Academic Publishers; 1976.) 57

5-6. Chromatic aberration. As a consequence of different refractions of rays of various wavelengths coming from a luminous point emitting mixed light, dispersion occurs for which the distance D is a measure. On the optical axis, a spectrum of image points will be formed, with points for violet (V) and red (R) at the extremities. (From James J. *Light Microscope Techniques in Biology and Medicine*. Dordrecht: Kluwer Academic Publishers; 1976.) 57

5-7. Basic components of a compound light microscope. (From James J. *Light Microscope Techniques in Biology and Medicine*. Dordrecht: Kluwer Academic Publishers; 1976.) 58

5-8. The effect of oil immersion. In situation I, without immersion, of three rays with an ever increasing angle toward the optical axis, only ray A reaches the objective in such a way that it can be presumed to take part in image formation, whereas ray C does not even reach the upper part of the object space, being totally reflected at the surface of the cover glass. In situation II, the same three rays reach the object space (virtually without being refracted) and both rays A′ and B′ probably can take part in image formation C′, reaching at least the upper part of the object space. It should be noted that the angles of ray A and B with the optical axis are greater than those of their counterparts A′ and B′). (From James J. *Light Microscope Techniques in Biology and Medicine*. Dordrecht: Kluwer Academic Publishers; 1976.) 59

5-9. Correction of chromatic aberration for two colors by the combination of a positive and a negative lens of materials with different dispersion; both image points come to coincide, but it entails an increase in the focal distance of the refractive complex. (From James J. *Light Microscope Techniques in Biology and Medicine*. Dordrecht: Kluwer Academic Publishers; 1976.) 60

5-10. **A:** Brightfield does not allow for viewing of cellular details, however **(B)** adjusting the aperture does allow for observation of details. (Modified from Hoffman R, Drewry J. *A Comparison of Four Types of Light Microscopy*. 5th ed. Dayton, OH: Educational Materials for Health Professionals; 2002.) 60

5-11. Phase contrast microscopy intensifies subtle contrasts. (Modified from Hoffman R, Drewry J. *A Comparison of Four Types of Light Microscopy*. 5th ed. Dayton, OH; Educational Materials for Health Professionals; 2002.) 61

5-12. Schematic view of the practical realization of the phase contrast principle; **(A)** phase annulus under the condenser **(B)** the corresponding phase plate in the objective. (From James J. *Light Microscope Techniques in Biology and Medicine*. Dordrecht: Kluwer Academic Publishers; 1976.) 61

5-13. **A:** Using a polarizing filter produces a blackened field of view; materials that polarize allow light to pass. **B:** A first order red compensation applied after polarization produces a red field of view, while polarized materials appear yellow or blue depending upon the orientation of the compensation filter. In this image the orientation of the compensator is in a neutral position. **C:** After adjusting the axis of the compensator filter, crystals aligned with the compensation filter appear yellow if negatively birefringent while crystals lying perpendicular to the filter appear blue, showing their positive birefringence. **D:** When the axis of the filter is flipped, the colors of the crystals reverse.

5-14. Schematic view of the development of a path difference when a light ray traverses a doubly refracting material, o, ordinary ray; e, extraordinary ray; Γ, path difference. (From James J, Tanke HJ, eds. *Biomedical Light Microscopy*. Dordrecht: Kluwer Academic Publishers; 1991.) 62

5-15. Schematic representation of the ray path in a light microscope adapted for modulation-contrast microscopy after Hoffman. (From James J, Tanke HJ, eds. *Biomedical Light Microscopy*. Dordrecht: Kluwer Academic Publishers; 1991.) 63

5-16. Modulation contrast microscopy creates a three-dimensional image. (Modified from Hoffman R, Drewry J. *A Comparison of Four Types of Light Microscopy*. 5th ed. Dayton, OH: Educational Materials for Health Professionals; 2002.) 63

5-17. Scheme of the course of interfering rays in differential interference contrast. W I and W II, Wollaston prisms; C, condenser; OB, object; 0, objective; EP, eyepiece. A polarizer in front of W I and analyzer behind W II are not shown. (From James J. *Light Microscope Techniques in Biology and Medicine*. Dordrecht: Kluwer Academic Publishers; 1976.) 64

5-18. Darkfield microscopy produces a bright image on a dark background. (Modified from Hoffman R, Drewry J. *A Comparison of Four Types of Light Microscopy*. 5th ed. Dayton, OH: Educational Materials for Health Professionals; 2002.) 64

5-19. Schematic view of the course of the rays in a vertical fluorescence illuminator with dichroic mirror. OB, object plane; BF, barrier filter; at right, a dark layer absorbing unused excitation light that has passed the

© Jones & Bartlett Learning LLC, an Ascend Learning Company. NOT FOR SALE OR DISTRIBUTION.

dichroic mirror. (From James J. *Light Microscope Techniques in Biology and Medicine*. Dordrecht: Kluwer Academic Publishers; 1976.) 64

5-20. Images show a high level of contrast when confocal microscopy is used in conjunction with fluorescence techniques. 65

5-21. Red blood cells as seen using a scanning electron microscope. 65

5-22. White blood cell as seen using a transmission electron microscope (call out shows this cell type viewed in brightfield microscopy with Wright stain). 65

5-23. Adjusting Kohler illumination **(A)** slide in focus for the objective to be used **(B)** misalignment of the condenser is made obvious when the field diaphragm is closed **(C)** properly centered condenser with closed field diaphragm **(D)** when the field diaphragm is opened, the light coming through a properly centered condenser fills the field evenly. 66

5-24. Proper microscope maintenance includes cleaning of lenses of the **(A)** oculars, **(B)** objectives, and **(C)** substage condenser with manufacturer recommended lens cleaner and lens paper. 67

6-1. Clean-catch urine collection kits include cleansing wipes. 73

6-2. Suprapubic aspiration of urine directly from the bladder. 74

6-3. The transfer of urine from collection containers **(A)** to testing tubes is made easy with the inclusion of a stopper-piercing port **(B and C).** Always ensure the transfer tube is labeled with the same patient identifiers as the primary specimen. 74

6-4. Transfer of urine from collection cups not having a port in their caps is made easier with the use of a sterile transfer device. 74

6-5. Use appropriate PPEs when transferring specimens from primary container to aliquot tubes. Always label the aliquot with the same patient identifiers as the primary container before transferring specimens. 74

6-6. Becton Dickensen urine tubes: **(A)** no additive urine tube; **(B)** chlorhexidine, along with other chemicals, is used to stabilize urine for routine testing for up to 72 hours; **(C)** boric acid is used for urine cultures; **(D)** special urine preservative tube (UPT) containing trademarked preservative suitable for molecular testing. 75

6-7. Male infant urine collection bag. 75

6-8. Cloth fibers (160×). 75

7-1. Urine specimens of varying normal colors. 80

7-2. Urine specimens from a patient with alkaptonuria **(A)** near fresh specimen; **(B)** turns black over time. 82

7-3. Urine specimens of varying abnormal colors and clarity. 82

7-4. Urine containing protein may produce a foam when agitated. 82

7-5. Schematic diagram of the total solids refractometer. (Courtesy of the American Optical Company, New York, NY, USA.) 85

7-6. Total solids refractometer using flow-through setup. 85

7-7. Schematic representation of the refractometer scales of measurement. This measurement represents a reading of 1.014. 85

7-8. Specific gravity color chart. (Modified from Tarrytown, NY: Bayer Corporation Diagnostics Division, 1996.) Note: this chart is for color demonstration only and should not be used for interpreting reagent strip reactions for diagnostic testing. 86

7-9. Image for questions 1 to 7. 86

8-1. **A:** Multistix 10 SG. **B:** Illustration of Multistix 10 SG with pad identification labels. (Modified from Siemens [formerly Bayer Corporation, Tarrytown NY]; 1996.)

8-2. Notice the discoloration of reagent pad (*arrow*) on this test strip that was exposed to moisture during storage (compare with Fig. 8-1A). 90

8-3. The reagent strip is dipped into a specimen and removed quickly, dragging the edge of the strip along the lip of the container to remove excess urine. 90

8-4. Follow the manufacturer's required times for reading of reagent strip test results. 91

8-5. Many companies exist worldwide who manufacture urine chemistry reagent strips. 91

8-6. pH color chart. Note: This chart is for color demonstration only and should not be used for interpreting reagent strip reactions for diagnostic testing. (Modified from Siemens Healthcare Diagnostics Inc. Tarrytown, NY; 2010). 91

8-7. The discoloration on the pH pad, due to improver removal of excess urine from the reagent test strip, causes a run-over effect of color change in the pH pad. 92

8-8. Protein color chart. Note: This chart is for color demonstration only and should not be used for interpreting reagent strip reactions for diagnostic testing. (Modified from Siemens Healthcare Diagnostics Inc. Tarrytown, NY; 2010). 93

8-9. Glucose color chart Note: This chart is for color demonstration only and should not be used for interpreting reagent strip reactions for diagnostic testing. (Modified from Siemens Healthcare Diagnostics Inc. Tarrytown, NY; 2010). 94

8-10. Clinitest reactions: Negative, 1+, 2+, 3+, and 4+. 95

8-11 Ketone color chart. Note: This chart is for color demonstration only and should not be used for interpreting reagent strip reactions for diagnostic testing. (Modified from Siemens Healthcare Diagnostics Inc. Tarrytown, NY; 2010). 96

8-12. Acetest color chart. Note: This chart is for color demonstration only and should not be used for interpreting reactions for diagnostic testing. (Modified from Siemens [formerly Elkhart, IN: Bayer HealthCare LLC]; 2006.) 97

8-13. Blood color chart. Note: This chart is for color demonstration only and should not be used for interpreting reagent strip reactions for diagnostic testing. (Modified from Siemens Healthcare Diagnostics Inc. Tarrytown, NY; 2010). 99

8-14. **A:** Normal pathway of bilirubin and urobilinogen metabolism; **(B)** pathway in hepatic jaundice; **(C)** pathway in obstructive jaundice; **(D)** pathway in hemolytic jaundice. 100

8-15. Bilirubin color chart. Note: This chart is for color demonstration only and should not be used for interpreting reagent strip reactions for diagnostic testing. (Modified from Siemens Healthcare Diagnostics Inc. Tarrytown, NY; 2010). 102

8-16. Ictotest color reactions. **A:** negative, **(B)** moderate, and **(C)** large. 103

8-17. ICTERO-CHECK test for urine bilirubin. (Courtesy of Biorex Labs LLC Cleveland, OH.) 103

8-18. Urobilinogen color chart. Note: This chart is for color demonstration only and should not be used for interpreting reagent strip reactions for diagnostic testing. (Modified from Siemens Healthcare Diagnostics Inc. Tarrytown, NY; 2010). 104

8-19. Nitrite color chart. Note: This chart is for color demonstration only and should not be used for interpreting reagent strip reactions for diagnostic testing. (Modified from Siemens Healthcare Diagnostics Inc. Tarrytown, NY; 2010). 105

8-20. Leukocyte esterase color chart. Note: This chart is for color demonstration only and should not be used for interpreting reagent strip reactions for diagnostic testing. (Modified from Siemens Healthcare Diagnostics Inc. Tarrytown, NY; 2010). 107

8-21. Ascorbic acid color chart. (Modified from Combi-Screen PLUS® [color chart]. Analyticon Biotechnologies AG, Lichtenfels, Germany; 2008.) 107

© Jones & Bartlett Learning LLC, an Ascend Learning Company. NOT FOR SALE OR DISTRIBUTION.

8-22. Calcium color chart. (Modified from UriTest 13G® Urine Reagent Strips [color chart]. Uritest Medical Electronic Co., Ltd. GuiLin, PR China; 2.) 107

8-23. Creatinine color chart. (Modified from UriTest 13G® Urine Reagent Strips [color chart]. Uritest Medical Electronic Co., Ltd. GuiLin, P.R China; 2006.) 108

8-24. Microalbumin color chart. (Modified from URS-3ACC® Reagent Strips for Urinalysis [color chart]. Jilin Shenhua Economic Trade Co., Ltd. 1188 Jinxin Street, Changchun, China.) 108

9-1. Kova system: **(A)** Kova Petter is inserted into a tube of centrifuged urine; and is used to decant, resuspend, and deliver sediment into one of the counting chambers; **(B)** Kova slide. Some models of Kova slides have 3-mm × 3-mm grids (as indicated by the call out). 112

9-2. Amorphous phosphates and hyaline cylindroid. The cylindroid is not visible in **A** but appears in **B** when the focus is adjusted (200×). 113

9-3. Red blood cells. The field also contains a white cell and several "ghost" cells (400×). 113

9.4 **A:** RBCs and WBCs. **B:** Changing the focus causes the red cells to appear as black circles (400×).

9-5. White blood cells in a hypotonic urine. The nuclei and granules are easily recognized (800×). 114

9-6. White cell clumps (200×). 115

9-7. Numerous white cells. Acetic acid (2%) was added to accentuate the nuclei (400×). 115

9.8 **A:** Transitional cell. **B:** Renal epithelial cells. **C:** WBCs (800×).

9-9. Transitional epithelial cells (500×). 116

9-10. Transitional epithelial cell (*large arrow*), several squamous epithelial cells, and white cells (200×) 116

9-11. Squamous epithelial cells (160×). 116

9-12. Spermatozoa (500×). 116

9-13. Bacteria (rods, cocci, and chains) (500×). 117

9-14. Yeast. Note the budding and doubly refractile walls (1,000×) 117

9-15. Schistosoma haematobium ovum. (Courtesy of Dr. Kenneth A. Borchardt, San Francisco State University, San Francisco, CA.) 117

9-16. Trichomonas vaginalis. Note the four flagella (1,000×). 117

9-17. Enterobius vermicularis ovum and WBCs (500×). 118

9-18. Head of Enterobius vermicularis adult female worm (1,000×) 118

9-19. Crystals frequently found in acidic urine. 118

9-20. Crystals less frequently found in acidic urine. 120

9-21. Calcium oxalate crystal (400×). 120

9-22. Calcium oxalate crystals. The "X" of each crystal is very prominent (500×). 120

9-23. Calcium oxalate crystals can sometimes appear as oval, dumbbells, and rosettes. 120

9-24. Uric acid: diamond or rhombic forms may also be referred to as "lemon-shaped" (500×). 121

9-25. Uric acid crystals in rosette formation (500×). 121

9-26. Uric acid: six-sided crystal may be confused with cystine (400×). 121

9-27. Uric acid: may display many colors under polarized light. Note the layered or laminated surface (400×). 121

9-28. Amorphous urates (200×). 121

9-29. Hippuric acid crystal (400×). 122

9-30. Sodium urate crystals. These needle-like crystals are not pointed at the ends (400×). 122

9-31. Cystine crystal (1,000×). 122

9-32. Cystine crystals. Several have laminated surfaces (160×). 122

9-33. Leucine spheroid. Note the radiating and concentric striations as well as the brown coloring typical of these crystals. 123

9-34. Leucine spheroid under polarized light. Notice the Maltese cross. (Modified from The Roche Historical Collection and Archive.) 123

9-35. Tyrosine crystals (160×). 123

9-36. Tyrosine crystals under polarized light. (Modified from The Roche Historical Collection and Archive.) 123

9-37. Cholesterol crystal with typical notched edges (250×). 124

9-38. Cholesterol crystal DIT microscopy. (Modified from The Roche Historical Collection and Archive.) 124

9-39. Esterified cholesterol polarizes light into a Maltese cross. Polarized light. (Modified from The Roche Historical Collection and Archive.) 124

9-40. Bilirubin crystals (500×). 124

9-41. Sulfonamide crystals, yeast, and WBCs. This photograph demonstrates two typical formations of sulfa crystals: the fan or sheaf formation and sheaves with eccentric bindings (400×). 125

9-42. X-ray dye crystals: Hypaque (160×). 125

9-43. X-ray dye crystals: Renografin (400×). 125

9-44. X-ray dye crystals may polarized light (160×). 125

9-45. Aspirin crystals—prismatic form. (Modified from The Roche Historical Collection and Archive.) 126

9-46. Aspirin crystals—stellate form. (Modified from The Roche Historical Collection and Archive.) 126

9-47. Acetophenetidin—stellate or "fir tree" forms. (Modified from The Roche Historical Collection and Archive.) 126

9-48. Ascorbic acid-spherulites (polarized light). (Modified from The Roche Historical Collection and Archive.) 126

9-49. Caffeine crystals (bright field) (Modified from The Roche Historical Collection and Archive.) 126

9-50. Crystals found in alkaline urine. 127

9-51. Triple phosphate crystals. Note the oblique ends of the prisms (200×). 127

9-52. Amorphous phosphate (400×). 127

9-53. Calcium carbonate crystals, spheroid and rhombohedral forms. (Modified from The Roche Historical Collection and Archive.) 127

9-54. Calcium carbonate crystals. The *small arrow* points out the typical "dumbbell" form which is next to a large mass of calcium carbonate crystals (400×). 128

9-55. Calcium phosphate crystals (400×). 128

9-56. Calcium phosphate plate or phosphate sheath (200×). 128

9-57. Ammonium biurate crystals (500×). 128

9-58. Ammonium biurate crystals without spicules (500×). 128

9-59. Sequence of urinary cast degeneration: (1) cellular casts; (2) coarse granular cast; (3) fine granular cast; (4) waxy cast. (Courtesy of Neil O. Hardy, Westpoint, CT.) 129

9-60. Hyaline cast and red blood cells. Note the low refractive index of the cast (400×). 130

9-61. Hyaline cast. (DIT microscopy) (600×). (Modified from The Roche Historical Collection and Archive.) 130

9-62. Red cell cast and RBCs (400×). 130

9-63. Red cell cast and RBCs (DIT microscopy) (400×). (Modified from The Roche Historical Collection and Archive.) 130

9-64. White cell cast and WBCs (500×). 130

© Jones & Bartlett Learning LLC, an Ascend Learning Company. NOT FOR SALE OR DISTRIBUTION.

9-65. Epithelial cell cast. (Phase) (800×). (Modified from The Roche Historical Collection and Archive.) 131
9-66. Epithelial cell cast. (DIT microscopy) (800×). (Modified from The Roche Historical Collection and Archive). 131
9-67. Coarsely granular cast (200×). 131
9-68. Finely granular casts. Note the RBCs between the two casts (500×). 131
9-69. Waxy cast, WBCs, and bacteria (400×). 132
9-70. Waxy cast and WBCs (200×). 132
9-71. Fatty cast (400×). 132
9-72. Fatty cast. (Polarization computer added) (400×). 132
9-73. Oval fat body and fiber (500×). 133
9-74. Fat droplets. Field also contains WBCs (500×). 133
9-75. Polarized anisotropic fat droplets. Note the "Maltese-cross" formation (160×). 133
9-76. Neutral fats and triglycerides stain with Sudan III, while esterified cholesterol remains colorless (400×). 133
9-77. Cylindroid. Note the tapering tail (400×). 134
9-78. Mucus (100×). 134
9-79. Starch crystal (500×). 134
9-80. Starch crystals. (Polarized light). Note the "Maltese-cross" formation (400×). 134
9-81. Cloth fibers (160×). 135
9-82. Fibers. Debris from a diaper. This squeezed-out specimen rendered microscopic examination useless. Note the various types of fibers present (200×). 135
9-83. This fiber is a common contaminant (400×). 135
9-84. This field of view shows an oil droplet (center), several WBCs and part of squamous cell (400×). 135
9-85. Hair **(right)** and coarsely granular cast **(left),** viewed using an 80A filter (400×). 136
9-86. Glass fragments are frequently present if a glass pipette is used to transfer sediment to the slide (400×). 136
9-87. Air bubble and amorphous urates (160×). 136
9-88. Talcum powder particles (160×). 136
9-89. Fecal contamination. The field also contains triple phosphate crystals (100×). 136
9-90. Image for Question 21. 137
9-91. Image for Question 22. 138
9-92. Image for Case Study 9-1. (Courtesy of Smith B, Foster KA. *The Urine Microscopic*. 5th ed. Educational Material for Health Professionals Inc; 1999.) 138
9-93. Image for Case Study 9-2. (Courtesy of Smith B, Foster KA. *The Urine Microscopic*. 5th ed. Educational Material for Health Professionals Inc; 1999.) 139
9-94. Image for Case Study 9-2. (Courtesy of Smith B, Foster KA. *The Urine Microscopic*. 5th ed. Educational Material for Health Professionals Inc; 1999.) 139
9-95. Image for Case Study 9-3. (Courtesy of Smith B, Foster KA. *The Urine Microscopic*. 5th ed. Educational Material for Health Professionals Inc; 1999.) 139
9-96. Image for Case Study 9-4. Unstained sediment. (Courtesy of Smith B, Foster KA. *The Urine Microscopic*. 5th ed. Educational Material for Health Professionals Inc; 1999.) 140
9-97. Image for Case Study 9-4 Sudan III-stained sediment. (Courtesy of Smith B, Foster KA. *The Urine Microscopic*. 5th ed. Educational Material for Health Professionals Inc; 1999.) 140
9-98. Image for Case Study 9-5. (Courtesy of Smith B, Foster KA. *The Urine Microscopic*. 5th ed. Educational Material for Health Professionals Inc; 1999.) 140

10-1. Hypotonic urine containing an RBC, several WBCs, two renal epithelial cells, and a transitional epithelial cell (500×). 143
10-2. Renal epithelial cells, WBCs, RBCs, and bacteria (500×). 143
10-3. Many RBCs and a squamous epithelial cell (160×). 143
10-4. SM-stained RBCs, some crenated (400×). (Courtesy of McBride LJ. *Textbook of Urinalysis and Body Fluids: A Clinical Approach*. Philadelphia, PA: Lippincott; 1998.) 143
10-5. Same field of view as previous under phase contrast microscopy (400×). (Courtesy of McBride LJ. *Textbook of Urinalysis and Body Fluids: A Clinical Approach*. Philadelphia, PA: Lippincott; 1998.) 143
10-6. WBCs, a few RBCs, and bacteria (500×). 143
10-7. SM-stained WBCs and bacteria under phase contrast microscopy (400×). (Courtesy of McBride LJ. *Textbook of Urinalysis and Body Fluids: A Clinical Approach*. Philadelphia, PA: Lippincott; 1998.) 144
10-8. Large clump of WBCs and many squamous epithelial cells (400×). 144
10-9. SM-stained RBCs, WBCs, and squamous epithelial cells (400×). (Courtesy of McBride LJ. *Textbook of Urinalysis and Body Fluids: A Clinical Approach*. Philadelphia, PA: Lippincott; 1998.) 144
10-10. Distorted WBCs. Acetic acid (2%) was added to the slide to accentuate the nuclei, thereby confirming that the distorted cells are WBCs. The reason for this distortion is unknown (400×). 144
10-11. Clump of WBCs, stained by bilirubin (200×). 144
10-12. WBCs and squamous epithelial cells (400×). 144
10-13. Renal epithelial cells (500×). 145
10-14. Sheet of squamous epithelial cells; most likely vaginal contamination (160×). 145
10-15. Numerous WBCs and few transitional cells (*arrow*) (200×). 145
10-16. SM-stained WBCs and transitional epithelial cells (200×). (Courtesy of McBride LJ. *Textbook of Urinalysis and Body Fluids: A Clinical Approach*. Philadelphia, PA: Lippincott; 1998.) 145
10-17. Squamous epithelial cells. 145
10-18. WBCs and bacteria. (Courtesy of Smith B, Foster KA. *The Urine Microscopic*. 5th ed. Educational Material for Health Professionals Inc.; 1999.) 145
10-19. SM-stained WBCs and bacteria (400×). (Courtesy of McBride LJ. *Textbook of Urinalysis and Body Fluids: A Clinical Approach*. Philadelphia, PA: Lippincott; 1998.) 146
10-20. Same field of view as previous figure under phase contrast microscopy (400×). (Courtesy of McBride LJ. *Textbook of Urinalysis and Body Fluids: A Clinical Approach*. Philadelphia, PA: Lippincott; 1998.) 146
10-21. Amorphous urates (100×). 146
10-22. Amorphous urates. The urates in this field are clumped close together. Note the characteristic color (100×). 146
10-23. Uric acid crystals, diamond or rhombic form. These crystals are very thin and almost colorless (400×). 146
10-24. Uric acid crystals in the urine of a patient with a kidney stone. Note the heavy clumps of crystals that were present, even in the fresh specimen (400×). 146
10-25. WBC cast and uric acid crystals. Same patient as in previous figure (400×). 147
10-26. Uric acid crystals in rosette formation (400×). 147
10-27. Uric acid crystals, atypical form (400×). 147
10-28. Uric acid crystals, layered formation (500×). 147
10-29. Uric acid crystals, thick rosette formation (200×). 147
10-30. Uric acid, thick rosette formation under higher power. Note the many layered crystals (500×). 147

© Jones & Bartlett Learning LLC, an Ascend Learning Company. NOT FOR SALE OR DISTRIBUTION.

10-31. Uric acid and calcium oxalate crystals (500×). 148
10-32. Uric acid crystals under polarized light. Note the small crystal (400×). 148
10-33. Uric acid under polarized light (400×). 148
10-34. Uric acid crystals (100×). (Courtesy of McBride LJ. *Textbook of Urinalysis and Body Fluids: A Clinical Approach*. Philadelphia, PA: Lippincott; 1998.) 148
10-35. Uric acid crystals (100×). (Courtesy of McBride LJ. *Textbook of Urinalysis and Body Fluids: A Clinical Approach*. Philadelphia: Lippincott, 1998.) 148
10-36. Uric acid crystals under polarized light (100×). (Courtesy of McBride LJ. *Textbook of Urinalysis and Body Fluids: A Clinical Approach*. Philadelphia, PA: Lippincott, 1998.) 148
10-37. Uric acid crystals under polarized light (100×). (Courtesy of McBride LJ. *Textbook of Urinalysis and Body Fluids: A Clinical Approach*. Philadelphia, PA: Lippincott; 1998.) 149
10-38. Uric acid crystals in pseudocast formation (400×). 149
10-39. Uric acid, barrel shape, and yeast in the background (200×). (Courtesy of McBride LJ. *Textbook of Urinalysis and Body Fluids: A Clinical Approach*. Philadelphia, PA: Lippincott; 1998.) 149
10-40. Sodium urate crystals. Note the square ends on each needle-like crystal (400×). 149
10-41. Sodium urates. Notice how narrow these crystals are (400×). 149
10-42. Sodium urate crystals (400×). 149
10-43. Uric acid, needle shape under polarized light with red compensator (400×). (Courtesy of McBride LJ. *Textbook of Urinalysis and Body Fluids: A Clinical Approach*. Philadelphia, PA: Lippincott; 1998.) 150
10-44. Calcium oxalate crystals (200×). 150
10-45. Calcium oxalate crystals. Even under low-power magnification, the characteristics of the crystals are easily recognized (160×). 150
10-46. Calcium oxalates, amorphous urates, and a piece of debris. Some of the crystals cracked when the coverslip was touched (200×). 150
10-47. Calcium oxalate crystals clustered around a piece of debris. The field also contains squamous epithelial cells as well at many calcium oxalates (100×). 150
10-48. Calcium oxalate forms seen in ethylene glycol poisoning. 150
10-49. More forms of calcium oxalate seen in ethylene glycol poisoning. 151
10-50. Hippuric acid crystals (400×). 151
10-51. Cystine crystals (160×). 151
10-52. Cystine crystal with unequal sides (1,000×). 151
10-53. Cystine crystals. Note how these crystals can form clusters (160×). 151
10-54. Cystine crystal with layered or laminated surface (1,000×). 151
10-55. Cystine crystals and a squamous epithelial cell. Some crystals have laminated surfaces and others are quite thick. The *arrow* shows a thick crystal that is turned on its edge (400×). 152
10-56. Leucine crystals. Note what appears to be a thick double wall and a striated center. 152
10-57. Leucine crystals under interference contrast microscopy. (Courtesy of Smith B, Foster KA. *The Urine Microscopic*. 5th ed. Educational Material for Health Professionals Inc.; 1999.) 152
10-58. Tyrosine crystals. Note how black the crystals appear on low power (160×). 152
10-59. Tyrosine crystals. Note the fine, very pointy needles (1,000×). 152
10-60. Tyrosine crystals (1,000×). 152
10-61. Tyrosine crystals under polarized light. (Courtesy of Smith B, Foster KA. *The Urine Microscopic*. 5th ed. Educational Material for Health Professionals Inc.; 1999.) 153
10-62. Tyrosine crystals (1,000×). 153
10-63. Cholesterol crystals from "kidney fluid" (200×). (Courtesy of McBride LJ. *Textbook of Urinalysis and Body Fluids: A Clinical Approach*. Philadelphia: Lippincott, 1998.) 153
10-64. Same specimen as the previous figure under polarized light. (Courtesy of McBride LJ. *Textbook of Urinalysis and Body Fluids: A Clinical Approach*. Philadelphia: Lippincott, 1998.) 153
10-65. X-ray dye crystals. Specific gravity of the specimen was 1.070 (160×). 153
10-66. X-ray dye crystals (400×). 153
10-67. X-ray dye crystals under polarized light (160×). 154
10-68. Bilirubin crystals and bilirubin-stained WBC and granular cast (500×). 154
10-69. Bilirubin crystals and bilirubin-stained sediment (500×). 154
10-71. Sulfonamide crystals (400×). (Courtesy of McBride LJ. *Textbook of Urinalysis and Body Fluids: A Clinical Approach*. Philadelphia, PA: Lippincott; 1998.) 154
10-70. Bilirubin crystals. (Courtesy of Smith B, Foster KA. *The Urine Microscopic*. 5th ed. Educational Material for Health Professionals Inc.; 1999.) 154
10-72. Sulfonamide crystals under polarized light with red compensator. (Courtesy of McBride LJ. *Textbook of Urinalysis and Body Fluids: A Clinical Approach*. Philadelphia, PA: Lippincott; 1998.) 154
10-73. Triple phosphate crystals. Many of these prisms are six-sided (200×). 155
10-74. Triple phosphate crystals and amorphous phosphates (200×). 155
10-75. Triple phosphate crystals (400×). 155
10-76. Triple phosphate crystals (500×). 155
10-77. Triple phosphates crystal and amorphous phosphates (200×). 155
10-78. Triple phosphate crystals under polarized light. (Courtesy of Smith B, Foster KA. *The Urine Microscopic*. 5th ed. Educational Material for Health Professionals Inc.; 1999.) 155
10-79. Triple phosphates crystal and amorphous phosphates. When crystals take on this grayish-black color, it usually means that they are beginning to dissolve (200×). 156
10-80. Triple phosphates crystal and amorphous phosphates. Note the unique formation of the center crystal (200×). 156
10-81. Triple phosphates crystal and mucus (400×). 156
10-82. Triple phosphate crystal. This crystal could be mistaken to be calcium oxalate, but the "X" does not cross exactly in the middle (400×). 156
10-83. Triple phosphate crystals under polarized light with red compensator (200×). (Courtesy of McBride LJ. *Textbook of Urinalysis and Body Fluids: A Clinical Approach*. Philadelphia, PA: Lippincott; 1998.) 156
10-84. Calcium phosphate crystals (400×). 156
10-85. Calcium phosphate plates and amorphous phosphates. Notice the thin granular plates (200×). 157
10-86. Calcium phosphate plate (or phosphate sheath) and amorphous phosphates (200×). 157
10-87. Ammonium biurate crystals (200×). 157

© Jones & Bartlett Learning LLC, an Ascend Learning Company. NOT FOR SALE OR DISTRIBUTION.

10-88. Ammonium biurate crystals (200×). 157
10-89. Ammonium biurate crystals (500×). 157
10-90. Ammonium biurate crystals (500×). 157
10-91. Ammonium biurate crystals (500×). 158
10-92. Ammonium biurate crystal and a squamous epithelial cell (500×). 158
10-93. Ammonium biurate crystals. These are the spheroid form of the crystal (500×). 158
10-94. Ammonium biurate crystals. Spheroid form without spicules (400×). 158
10-95. Ammonium biurate crystals (500×). 158
10-96. Hyaline cast, WBCs, RBCs, and bacteria. Can you see the bent cast? (500×). 159
10-97. Hyaline casts. How many casts can you find? (200×). 159
10-98. Hyaline cast that is bent back upon itself and many RBCs. Viewed with an 80A filter (400×). 159
10-99. Hyaline casts. Viewed with an 80A filter (400×). 159
10-100. Hyaline casts using phase contrast microscopy. (Courtesy of Smith B, Foster KA. *The Urine Microscopic*. 5th ed. Educational Material for Health Professionals Inc.; 1999.) 159
10-101. Many hyaline casts and WBC casts and rare RBC (200×). 159
10-102. Hyaline cast, WBCs, RBCs, and epithelial cells (200×). 160
10-103. Hyaline cast with a few granular inclusions (500×). 160
10-104. Convoluted red blood cell cast (500×). 160
10-105. Red blood cell cast and many RBCs. The cells in the cast are still intact (500×). 160
10-106. Red blood cell cast. There are still some intact cells in the cast (*arrow*), although many of the cells have begun to degenerate (500×). 160
10-107. Red blood cell cast. When the cast in the previous figure is viewed under low power, the color of the cast is more prominent (200×). 160
10-108. Red blood cell cast and amorphous urates (500×). 161
10-109. White blood cell cast, WBCs, squamous epithelial cells, and mucus (400×). 161
10-110. White blood cell cast. The protein matrix is clearly visible (500×). 161
10-111. SM-stained WBC cast (400×). (Courtesy of McBride LJ. *Textbook of Urinalysis and Body Fluids: A Clinical Approach*. Philadelphia: Lippincott, 1998.) 161
10-112. White blood cell cast (400×). 161
10-113. Bilirubin-stained casts, fibers, and sediment (200×). 161
10-114. Mixed cell cast, WBCs, and RBCs. This cast contains degenerating WBCs and several RBCs (500×). 162
10-115. Bilirubin-stained WBC cast. Bilirubin staining can cause problems in identifying structures, but you can see some cell outlines. In addition, the WBCs are beginning to degenerate, creating a granular cast appearance (500×). 162
10-116. Many WBC casts and many WBCs (200×). 162
10-117. SM-stained mixed cellular cast including renal tubular epithelial cells (400×). (Courtesy of McBride LJ. *Textbook of Urinalysis and Body Fluids: A Clinical Approach*. Philadelphia, PA: Lippincott; 1998.) 162
10-118. Epithelial cell cast. The nuclei are visible in some of the cells (500×). 162
10-119. Mixed cast. This cast is half hyaline and half granular. Report as "hyaline" and/or "granular," but not "mixed" cast (400×). 162
10-120. Mixed cast, yeast, and a WBC. This cast is also half hyaline and half granular (500×). 163
10-121. Mixed cast. Note bacteria in one-half of the cast. Bacterial casts are not very common (500×). 163
10-122. Many casts, WBCs, RBCs, and amorphous sediment, all of which are stained with bilirubin (200×). 163
10-123. Broad mixed granular and RBC cast, and a broad granular cast. Higher magnification of previous figure. This specimen is from a patient with Wilson disease (500×). 163
10-124. SM-stained hyaline cast, granular cast, mixed cellular cast, and partially degenerated renal tubule epithelial cells (200×). (Courtesy of McBride LJ. *Textbook of Urinalysis and Body Fluids: A Clinical Approach*. Philadelphia, PA: Lippincott; 1998.) 163
10-125. Broad granular cast (400×). 163
10-126. Fine granular cast, WBCs, and RBCs (500×). 164
10-127. Fine granular casts and WBCs. Note the smaller cast (500×). 164
10-128. SM-stained granular cast (200×). (Courtesy of McBride LJ. *Textbook of Urinalysis and Body Fluids: A Clinical Approach*. Philadelphia, PA: Lippincott; 1998.) 164
10-129. Fine granular casts and WBCs (400×). 164
10-130. Coarse granular cast (500×). 164
10-131. Coarse granular cast (400×). 164
10-132. Coarse granular cast, calcium phosphate plate, and amorphous phosphates (200×). 165
10-133. Broad and narrow coarse granular casts (200×). 165
10-134. Coarse granular cast (400×). 165
10-135. Bilirubin-stained granular cast (500×). 165
10-136. Fine granular cast (400×). 165
10-137. Fine granular cast, WBCs, and bacteria (400×). 165
10-138. Waxy cast and amorphous urates. Note the indentations on the sides of the cast (500×). 166
10-139. Bilirubin-stained waxy cast, granular cast, WBCs, and amorphous sediment. Note the convolutions near the center of the waxy cast (500×). 166
10-140. Long waxy cast, WBCs, and an epithelial cell. The surface of this cast is more refractile than that of a hyaline cast (200×). 166
10-141. Fine granular cast becoming a waxy cast. This cast would best be classified as a waxy cast, because of the typical cracks on the sides of this cast, even though the surface is still granular (500×). 166
10-142. Convoluted waxy cast. This field also contains WBCs, rare RBC, and bacteria (500×). 166
10-143. Convoluted waxy cast. This is the same image as the previous figure, but when the fine adjustment is turned slightly, the cast seems to develop a dark edge because of the high refractive index of the cast (500×). 166
10-144. SM-stained waxy cast (100×). (Courtesy of McBride LJ. *Textbook of Urinalysis and Body Fluids: A Clinical Approach*. Philadelphia, PA: Lippincott; 1998.) 167
10-145. Same field as previous figure using phase contrast microscopy (100×). (Courtesy of McBride LJ. *Textbook of Urinalysis and Body Fluids: A Clinical Approach*. Philadelphia, PA: Lippincott; 1998.) 167
10-146. SM-stained waxy-granular cast (200×). (Courtesy of McBride LJ. *Textbook of Urinalysis and Body Fluids: A Clinical Approach*. Philadelphia, PA: Lippincott; 1998.) 167
10-147. Granular cylindroid (500×). 167
10-148. Hyaline cylindroid. Note the tapering tail (160×). 167
10-149. Fine granular cast and yeast (400×). 168

© Jones & Bartlett Learning LLC, an Ascend Learning Company. NOT FOR SALE OR DISTRIBUTION.

10-150. Bacteria. This field contains rods, cocci, and chains (500×). 168

10-151. Yeast, WBCs, rare RBC, and bacteria (500×). 168

10-152. Yeast (1,000×). 168

10-153. SM-stained yeast with pseudohyphae and WBCs (200×). (Courtesy of McBride LJ. *Textbook of Urinalysis and Body Fluids: A Clinical Approach*. Philadelphia, PA: Lippincott; 1998.) 168

10-154. Yeast under phase contrast microscopy (400×). (Courtesy of McBride LJ. *Textbook of Urinalysis and Body Fluids: A Clinical Approach*. Philadelphia, PA: Lippincott; 1998.) 168

10-155. Pinworm ovum and WBCs (100×). The characteristics of the pinworm ovum are easily recognized, even under low-power magnification. 169

10-156. *Enterobius vermicularis* or pinworm ovum (400×). 169

10-157. Tail of the adult female pinworm. The tail of the female is straight and very pointed, whereas the tail of the male is curved (40×). 169

10-158. Pinworm ovum and WBCs (500×). 169

10-159. *Schistosoma haematobium* ovum under interference contrast microscopy. (Courtesy of Smith B, Foster KA. *The Urine Microscopic*. 5th ed. Educational Material for Health Professionals Inc.; 1999.) 169

10-160. *Trichomonas vaginalis* with mixed cellular background viewed under phase contrast microscopy. (Courtesy of McBride LJ. *Textbook of Urinalysis and Body Fluids: A Clinical Approach*. Philadelphia: Lippincott, 1998.) 169

10-161. Sperm and epithelial cells (500×). 170

10-162. Sperm (wet-mount). 170

10-163. Mucus. (Courtesy of Smith B, Foster KA. *The Urine Microscopic*. 5th ed. Educational Material for Health Professionals Inc.; 1999.) 170

10-164. Mucus containing WBCs and RBCs (200×). 170

10-165. Fat droplets and epithelial cells (160×). 170

10-166. Oval fat body, granular cast, and amorphous urates. The oval fat body contains only a few fat droplets, thus, having a smaller size than other fat bodies (500×). 170

10-167. Oval fat body (400×). 171

10-168. Oval fat body. The cell is bulging with fat droplets, so the cell membrane is not visible (500×). 171

10-169. Oval fat bodies and WBCs (500×). 171

10-170. Oval fat body. This field also contains a cell with a few small fat droplets in it (*arrow*) (400×). 171

10-171. Sudan III-stained fat droplets. (Courtesy of Smith B, Foster KA. *The Urine Microscopic*. 5th ed. Educational Material for Health Professionals Inc.; 1999.) 171

10-172. Starch granules (200×). 171

10-173. Starch crystals. The indentation in the center of each crystal is very distinguishable (500×). 172

10-174. Starch granules. (Courtesy of McBride LJ. *Textbook of Urinalysis and Body Fluids: A Clinical Approach*. Philadelphia, PA: Lippincott; 1998.) 172

10-175. Starch crystals under polarized light demonstrating the typical "Maltese-cross" formation (400×). 172

10-176. Talcum powder particles and a few squamous epithelial cells (160×). 172

10-177. Debris from a diaper. The piece of debris in the center of the field is a common contaminant (400×). 172

10-178. **A:** Fine granular cast and WBCs. Note the detail of the cast. **B:** Fiber. Note the dark edges and the difference in texture between this piece of debris and the cast in **(A)** (200×).

10-179. Fiber. Note the dark edges (400×). 173

10-180. Fiber. This fiber could be confused with a waxy cast, but the structure is determined to be flat because of the part of the fiber that is turned on its side (400×). 173

10-181. Fiber. Note the thick rolled edges of this fiber (400×). 173

10-182. Debris from a diaper. This squeezed-out specimen was worthless for microscopic analysis. Note the various types of fibers present (200×). 173

10-183. Fibers. The striations (seen only under low-power magnification) and dark edges are characteristics of these fibers (400×). 174

10-184. Fibers. These are the same fibers as in the previous figure. Note the indentations in the surface of the center fiber (400×). 174

10-185. Fiber. Note the nodular indentations and nodular end of this very common contaminant (400×). 174

10-186. Fibers. The center fiber shows a thick nodular border (500×). 174

10-187. Fiber, calcium oxalate crystals, and amorphous urates. Note the nodular ends on the fiber (400×). 174

10-188. Fiber. This is the same field as in the previous figure but on a different focal plane. Changing the focus brings out the nodular indentations on the side of the fiber (400×). 174

10-189. Air bubbles, phosphate plate, and amorphous phosphates. Air bubbles can assume a variety of shapes, especially if the coverslip is moved or depressed (200×). 175

10-190. Coverslip defects. (Courtesy of Smith B, Foster KA. *The Urine Microscopic*. 5th ed. Educational Material for Health Professionals Inc.; 1999.) 175

11-1. Forces governing the exchange of fluid at the capillary level. 179

11-2. Exchanges through capillary membranes in the formation and removal of interstitial fluid. 180

11-3. Neubauer hemocytometer diagrams. (Modified from Spahn MA, Brackman E. *Manual Cell Counting Techniques*. Dayton, OH: Educational Materials for Health Professional Inc.; 1987) 181

11-4. Cytocentrifuge. 182

11-5. Cytocentrifugation method of body fluid concentration. An assembly of a special cuvette, with attached filter paper, and a glass slide are clipped into place in the cytocentrifuge. One to two drops of well-mixed fluid are pipetted into the cuvette. The lids are closed and the sample is centrifuged at 500 rpm for 5 minutes. 182

11-6. Cytocentrifuge-prepared smears are marked with a wax pencil to outline the area of cell deposit. Smears are stained with Wright stain for microscopic evaluation. 182

12-1. Anatomy of the central nervous system. From Snell R. *Clinical Neuroanatomy*. Burlington, MA: Jones & Bartlett Learning, LLC; 2001. 186

12-2. Detail of meninges. From Cormack DH. *Ham's Histology*. 9th ed. Philadelphia, PA: J. B. Lippincott; 1987:367. 186

12-3. Placement of the needle for CSF collection. (Courtesy of Wolters Kluwer, Skokie, IL.) 187

12-4. Specimen containers for cerebral spinal fluid specimens. 187

12-5. Comparison of cerebral spinal fluid appearance between **(A)** normal CSF, **(B)** red CSF from fresh hemorrhage, **(C)** xanthochromic CSF from old hemorrhage, and **(D)** CSF from a traumatic tap. 188

12-6. Cells that can normally be found in cerebral spinal fluid. **(A)** Neutrophil, **(B)** monocyte, and **(C)** lymphocytes. Red blood cells are not normally present in CSF (Wright stain 1,000×). 188

© Jones & Bartlett Learning LLC, an Ascend Learning Company. NOT FOR SALE OR DISTRIBUTION.

12-7. Neutrophilic pleocytosis in cerebral spinal fluid (Wright stain 1,000×). 189

12-8. Lymphocytic pleocytosis in cerebral spinal fluid (Wright stain 1,000×). 190

12-9. Plasma cells in cerebral spinal fluid (Wright stain 1,000×). 190

12-10. Eosinophils in cerebral spinal fluid (Wright stain 1,000×). 190

12-11. Cerebral spinal fluid with mixed pleocytosis (Wright stain 1,000×). 190

12-12. Macrophage in cerebral spinal fluid (Wright stain 1,000×). 191

12-13. Macrophage demonstrating erythrophagocytosis in cerebral spinal fluid can be seen 12 to 48 hours following CNS hemorrhage (Wright stain 1,000×). 191

12-14. Macrophage demonstrating erythrophagocytosis in cerebral spinal fluid can be seen along with siderotic granules 2 to 4 days following CNS hemorrhage (Wright stain 1,000×). 191

12-15. Macrophage with iron inclusions (siderophage) in cerebral spinal fluid can be seen from 1 to 8 following CNS hemorrhage (Wright stain 1,000×). 192

12-16. Macrophage with hematin inclusions (arrows) in cerebral spinal fluid (Wright stain 1,000×). 192

12-17. Macrophages with possible fat inclusions (lipophage) in cerebral spinal fluid (Wright stain 1,000×). 192

12-18. Ependymal cells in cerebral spinal fluid (Wright stain 1,000×). 192

12-19. Clumped choroid plexus in cerebral spinal fluid (Wright stain 1,000×). 192

12-20. Cells of lymphocyte lineage may be seen in CSF from patients with lymphocytic leukemias (Wright stain 1,000×). 192

12-21. Nucleated red blood cells in cerebral spinal fluid are usually due to a traumatic tap (Wright stain 1,000×). 193

12-22. Squamous epithelial cells are rarely found in CSF and are contaminants introduced during the lumbar puncture procedure. This field of view also contains five neutrophils (Wright stain 1000×). 193

12-23. Comparison of Wright-stained and Gram-stained bacteria in cerebral spinal fluid. **A:** Wright stain (notice bacteria stain blue). **B:** Gram stain reveals that the bacteria are gram-negative (*pink*). 195

12-24. Positive India ink stain. (Courtesy of Wolters Kluwer.) 195

12-25. Case 12-1 Wright-stained cytocentrifuged CSF. 197

12-26. Case 12-2 CSF specimen tubes one, two, and three. 197

12-27. Case 12-3 Wright-stained cytocentrifuged CSF. 197

12-28. Case 12-3 CSF specimen tubes 1, 2, and 3. 198

12-29. Case 12-3 Wright-stained cytocentrifuged CSF. 198

13-1. Mesothelial lining of serous body cavities. (Image courtesy of Wolters Kluwer, Skokie, IL.) 200

13-2. Colors of serous fluids: **(A)** normal; **(B)** red/bloody; **(C)** milky/chylous; **(D)** greenish-brown. 200

13-3. Cytospin preparation of pleural fluid containing RBCs and lymphocytes in acute inflammation. Wright stain (400×). (Image courtesy of McBride LJ. *Textbook of Urinalysis and Body Fluids: A Clinical Approach*. Philadelphia, PA: Lippincott; 1998.) 201

13-4. Cytospin preparation of pleural fluid containing RBCs, neutrophils, and a mesothelial cell in bacterial infection. Wright stain (200×). (Image courtesy of McBride LJ. *Textbook of Urinalysis and Body Fluids: A Clinical Approach*. Philadelphia, PA: Lippincott; 1998.) 201

13-5. Cytospin preparation of peritoneal fluid containing RBCs, lymphocytes, monocytes, and mesothelial cells. Wright stain (200×). (Image courtesy of McBride LJ. *Textbook of Urinalysis and Body Fluids: A Clinical Approach*. Philadelphia, PA: Lippincott; 1998.) 201

13-6. Cytospin preparation of pericardial fluid containing RBCs, WBCs, and cells resembling adenocarcinoma. Wright stain (200×). (Image courtesy of McBride LJ. *Textbook of Urinalysis and Body Fluids: A Clinical Approach*. Philadelphia, PA: Lippincott; 1998.) 202

13-7. Cytospin preparation of pleural fluid containing RBCs, macrophages. Wright stain (800×). 202

13-8. Cytospin preparation of pleural fluid containing neutrophils. Wright stain (800×). 202

13-9. Cytospin preparation of ascites fluid containing RBCs, plasmacells from a patient with multiple myeloma. Wright stain (800×). 202

13-10. Cytospin preparation of ascites fluid containing RBCs, mesothelial cells. Wright stain (800×). 202

13-11. Cytospin preparation of peritoneal fluid containing RBCs, WBCs, and many bacteria. Identified by culture as *Escherichia coli*. Wright stain (1,000×). (Image courtesy of McBride LJ. *Textbook of Urinalysis and Body Fluids: A Clinical Approach*. Philadelphia, PA: Lippincott; 1998.) 202

13-12. Cytospin preparation of peritoneal fluid containing WBCs and few bacteria. Identified by culture as Staphylococcus. Wright stain (1,000×). (Image courtesy of McBride LJ. *Textbook of Urinalysis and Body Fluids: A Clinical Approach*. Philadelphia, PA: Lippincott; 1998.) 203

13-13. Cholesterol crystals in pleural fluid. Bright light (400×). 203

13-14. Cholesterol crystals in pleural fluid. **A:** Polarized light. **B:** Polarized, compensated light (400×). 204

13-15. The heart and pericardium. (Asset provided by Anatomical Chart Co, Skokie, IL.) 205

13-16. Aspirating pericardial fluid. In pericardiocentesis, a needle and syringe are inserted through the chest wall into the pericardial sac (as shown below). Electrocardiographic monitoring, with a lead wire attached to the needle and electrodes placed on the limbs (right arm, left arm, and left leg), helps ensure proper needle placement and avoids damage to the heart. (From *Nursing Procedures*. 4th ed. Ambler, PA: Lippincott Williams & Wilkins; 2004.) 206

13-17. The pleural cavity with effusion. (From Cohen BJ. *Medical Terminology*. 4th ed. Burlington, MA: Jones & Bartlett Learning, LLC; 2003). 207

13-18. Thoracentesis. A needle is inserted into the pleural space to withdraw fluid. (From Cohen BJ. *Medical Terminology*. 4th ed. Burlington, MA: Jones & Bartlett Learning, LLC; 2004.) 207

13-19. The organs of the abdomen. IVC, inferior vena cava. (From Moore KL, Agur A. *Essential Clinical Anatomy*. 2nd ed. Philadelphia, PA: Lippincott Williams & Wilkins; 2002.) 208

13-20. Paracentesis of the abdominal cavity in midline. (From Snell RS. *Clinical Anatomy*. 7th ed. Lippincott Williams & Wilkins; 2003.) 208

13-21. Wright stain of ascites fluid. (Image courtesy of McBride LJ. *Textbook of Urinalysis and Body Fluids: A Clinical Approach*. Philadelphia, PA: Lippincott; 1998.) 209

13-22. Pleural fluid. 210

14-1. Articulated joint. (From Oatis CA. *Kinesiology: The Mechanics and Pathomechanics of Human Movement*. Baltimore, MD: Lippincott Williams & Wilkins; 2003.) 212

© Jones & Bartlett Learning LLC, an Ascend Learning Company. NOT FOR SALE OR DISTRIBUTION.

14-2. Synovial membrane from a normal knee joint shows joint space, synovial membrane composed of synovial cells embedded in a loose connective tissue stroma overlying dense collagen (hematoxylin and eosin). (From McClatchey KD. *Clinical Laboratory Medicine*. 2nd ed. Philadelphia, PA: Lippincott Williams & Wilkins; 2002.) 212

14-3. Bulge test of joint for the detection of synovial effusion. 212

14-4. Placement of needle in arthrocentesis of **(A)** elbow and **(B)** knee joints. 213

14-5. Synovial fluid. **A:** Normal. **B:** Bloody. 213

14-6. Synovial fluid inclusions. **A:** "Ground pepper" ochronotic shards. **B:** "Rice bodies" fibrin-enriched synovium fragments. 214

14-7. String test showing normal synovial fluid viscosity. 214

14-8. Mucin clot test of normal synovial fluid. 215

14-9. Normal cellular elements found in synovial fluid include **(A)** neutrophils, **(B)** lymphocytes, **(C)** monocytes/histiocytes, and **(D)** synovial lining cells. A few red blood cells are almost always present in joint effusions (Wright–Giemsa). (From McClatchey KD. *Clinical Laboratory Medicine*. 2nd ed. Philadelphia, PA: Lippincott Williams & Wilkins; 2002.) 216

14-10. Synovial fluid with acute inflammation demonstrating neutrophilic pleocytosis (Wright–Giemsa). (From McClatchey KD. *Clinical Laboratory Medicine*. 2nd ed. Philadelphia, PA: Lippincott Williams & Wilkins, 2002.) 216

14-11. LE cell (*arrow*) is a neutrophil containing a phagocytized homogeneous nucleus (Wright–Giemsa). (From McClatchey KD. *Clinical Laboratory Medicine*. 2nd ed. Philadelphia, PA: Lippincott Williams & Wilkins; 2002.) 216

14-12. Tart cell: a macrophage containing a phagocytized nucleus that retains some nuclear detail (Wright–Giemsa). (From McClatchey KD. *Clinical Laboratory Medicine*. 2nd ed. Philadelphia, PA: Lippincott Williams & Wilkins; 2002.) 216

14-13. Reiter cell (center) is a macrophage that has phagocytosed one or more neutrophils. This finding is not specific for Reiter syndrome. (From McClatchey KD. *Clinical Laboratory Medicine*. 2nd ed. Philadelphia, PA: Lippincott Williams & Wilkins; 2002.) 217

14-14. Lipid-laden macrophage in synovial fluid (Wright–Giemsa). (From McClatchey KD. *Clinical Laboratory Medicine*. 2nd ed. Philadelphia, PA: Lippincott Williams & Wilkins, 2002.) 217

14-15. Synovial fluid with acute inflammation and monosodium urate crystals. (Wright–Giemsa stain and polarized light). (From McClatchey KD. *Clinical Laboratory Medicine*. 2nd ed. Philadelphia, PA: Lippincott Williams & Wilkins; 2002.) 217

14-16. Synovial fluid with acute inflammation and monosodium urate crystals. The needle-shaped crystals demonstrate negative birefringence, because they are yellow when aligned with the compensator filter and blue when perpendicular to the filter (Wright–Giemsa stain and polarized/compensated light). (From McClatchey KD. *Clinical Laboratory Medicine*. 2nd ed. Philadelphia, PA: Lippincott Williams & Wilkins; 2002.) 217

14-17. Synovial fluid with acute inflammation and calcium pyrophosphate dihydrate crystals (Wright–Giemsa stain and polarized light). (From McClatchey KD. *Clinical Laboratory Medicine*. 2nd ed. Philadelphia, PA: Lippincott Williams & Wilkins; 2002.) 217

14-18. Synovial fluid with acute inflammation and calcium pyrophosphate dihydrate crystals. The rhomboidal intracellular crystal (center) demonstrates positive birefringence, because it is blue when aligned with the compensator filter (Wright–Giemsa stain and polarized/compensated light). (From McClatchey KD. *Clinical Laboratory Medicine*. 2nd ed. Philadelphia, PA: Lippincott Williams & Wilkins; 2002.) 217

14-19. First image for Case Study 14-1. Synovial fluid. 219

14-20. Second image for Case Study 14-1. (From McClatchey KD. *Clinical Laboratory Medicine*. 2nd ed. Philadelphia, PA: Lippincott Williams & Wilkins; 2002.) 220

14-21. First image for Case Study. Synovial fluid. 220

14-22. Second image for Case Study 14-2. (Courtesy of McBride LJ. *Textbook of Urinalysis and Body Fluids: A Clinical Approach*. Philadelphia, PA: Lippincott; 1998.) 220

15-1. Diagram of alimentary tract. 222

15-2. Gastric contents collection using nasogastric intubation and aspiration. 223

15-3. Gastroccult test card with interpretation. **A:** Cover of closed Gastroccult card. **B:** Gastroccult test card opened with positive test result. **C:** Interpretation of Gastroccult results. (Images courtesy of Beckman Coulter, Inc.) 224

15-4. Fecal leukocytes. **A:** Gram stain, (1,000×), fecal leukocytes. **B:** Wright stain (1,000×), fecal leukocytes. **C:** Wet preparation, Shigella dysentery or bacterial dysentery with fecal white blood cells, red blood cells, and bacteria. (Fig. 15-4C obtained from: http://phil.cdc.gov/phil image 6659.) 225

15-5. Hemoccult positive fecal occult blood test. (Courtesy of Beckman Coulter, Inc.) 226

15-6. Hemoccult-ICT positive fecal occult blood test. (Courtesy of Beckman Coulter, Inc.) 226

15-7. Steatorrhea with fecal fat Sudan III stain for neutral fats. 227

15-8. Steatorrhea with fecal fat Sudan III stain for fatty acids. 227

15-9. Creatorrhea. Undigested meat fiber. Note the clearly defined muscle striations. 228

15-10. Creatorrhea. Undigested meat fibers tangled. The clear striations help identify these meat fibers. 228

16-1. Detail of the male reproductive system. (Reprinted with permission from Cohen BJ, Wood DL. *Memmler's the Human Body in Health and Disease*. 9th ed. Burlington, MA: Jones & Bartlett Learning, LLC, 2000.) 232

16-2. The process of spermatogenesis in the seminiferous tubules. (Courtesy of Wolter Kluwer, Skokie, IL.) 233

16-3. Final stages of spermatogenesis. **A:** Immature spermatid with round shaped nucleus, early signs of acrosome and tail development; **B:** Immature spermatid with formation of the acrosome, nuclear condensation developing tail piece; **C:** Spermatid with acrosome covering the nucleus, developing middle piece, and shrinking cytoplasmic membrane; **D:** Mature spermatozoon. (Courtesy of Wolter Kluwer, Skokie, IL.) 233

16-4. Normal semen viscosity test. 235

16-5. Inclusion criteria of counting cells. Count cells (sperm heads, not tails) that touch the upper and left boarders of the counting grid. Do not count cells (sperm heads, not tails) that touch the lower and right boarders of the counting grid. Count only complete sperm. 235

16-6. Wet mount of semen. Many sperm are present (450×). (Courtesy of Hapner and Spahn, Dayton, OH: Educational Materials for Health Professional Inc., 1981.) 236

16-7. Wet mount of semen. Several sperm can be seen along with a red blood cells (R) and a white blood cell (W) (450×). (Courtesy of Hapner and Spahn.) 236

16-8. Viable sperm do not take up the eosin stain and remain colorless, thus appearing white (eosin/nigrosin stain, 1,000×). 237

16-9. Nonviable sperm take up the eosin stain and appear various shades of red (eosin/nigrosin stain, 1,000×). 237

© Jones & Bartlett Learning LLC, an Ascend Learning Company. NOT FOR SALE OR DISTRIBUTION.

16-10. Features of a normal spermatozoon. (Courtesy of Wolter Kluwer, Skokie, IL.) 238

16-11. Normal sperm (Papanicolaou stain, 1,000×). 238

16-12. Normal sperm. The arrow points to a sperm observed with a side view (Papanicolaou stain, 1,000×). 238

16-13. Normal sperm, side view (Papanicolaou stain, 1,000×). 238

16-14. Double-headed sperm. Notice the excessive cytoplasmic membrane in image C (Papanicolaou stain, 1,000×). 238

16-15. Double-tailed sperm. Arrows point to both tails. (Papanicolaou stain, 1,000×). 239

16-16. Coiled-tailed sperm. Tails may coil completely around the head as seen in image A (Papanicolaou stain, 1,000×). 239

16-17. Flat-headed sperm. One normal sperm is seen among those with flat heads, indicating the absence of the acrosomal cap (Papanicolaou stain, 1,000×). 239

16-18. Various sperm head sizes. **A:** Normal sperm. **B:** Large head. **C:** Small or pinhead (Papanicolaou stain, 1,000×). 239

16-19. Normal sperm shown with sperm at arrow that has a constricted (or pinched) head and excessive cytoplasmic membrane (Papanicolaou stain, 1,000×). 240

16-20. Various sperm anomalies. **A:** Normal sperm. **B:** Sperm with constricted (or pinched) head and excessive cytoplasmic. 240

16-21. These sperm both have bent neck pieces. One has a normal head, whereas the other is a pinhead (Papanicolaou stain, 1,000×). 240

16-22. These sperm have round heads rather than oval (Papanicolaou stain, 1,000×). 240

16-23. These sperm all have tapered heads rather than oval. Image B also shows excessive cytoplasmic membrane and image C has a coiled tail (Papanicolaou stain, 1,000×). 241

16-24. The heads of these sperm all contain vacuoles (Papanicolaou stain, 1,000×). 241

16-25. The necks of these sperm have excessive cytoplasmic membrane remaining (Papanicolaou stain, 1,000×). 241

16-26. Immature spermatids (Papanicolaou stain, 1,000×). 241

16-27. Figure for review questions 16 to 18. 244

17-1. Schematic drawing of the amniotic cavity. (Nath JL. *Using Medical Terminology: A Practical Approach*. Burlington, MA: Jones & Bartlett Learning, LLC; 2006.) 247

17-2. Potter complex results from leakage of amniotic fluid, oligohydramnios. Congenital hydronephrosis results from urinary tract obstruction. 248

17-3. Amniocentesis is performed under ultrasound guidance. A needle is inserted through the mother's abdomen into a pocket of amniotic fluid, which is then aspirated with a syringe. 248

17-4. Numerous squamous epithelial cells, and other cells observed in cytocentrifuge preparation of amniotic fluid. Wright stain 200×. (Courtesy of McBride, *Textbook of Urinalysis and Body Fluids.* LWW; 1998.) 249

17-5. Spectrophotometric scan of amniotic fluid indicating bilirubin and oxyhemoglobin peaks. Note the near linearity of the normal curve in A. In B, note the elevated bilirubin peak (at 450 nm) and the oxyhemoglobin peak (at 410 nm). The base is drawn from 550 nm to 365 nm. (From Burtis CA, Ashwood ER. *Tietz Textbook of Clinical Chemistry*. 2nd ed. Philadelphia, PA: WB Saunders Company; 1994.) 250

17-6. Liley graph for assessment of fetal risk. The Liley graph is a three-zone chart with modification for the interpretation of amniotic fluid change in absorbance at 450 nm versus weeks of gestation. The graph divides the patient's readings into three zones of gestational risk, with zone III posing the greatest risk for the developing infant. (From Burtis CA, Ashwood ER. *Tietz Textbook of Clinical Chemistry*. 2nd ed. Philadelphia, PA: WB Saunders Company; 1994.) 251

18-1. **A:** A warmed speculum allows for visualization and insertion of swab. **B:** The swab is used to sample the vaginal pool and nontraumatically "scrape" the cervical os and walls of the vagina (depending on test requirements).

18-2. "Ferning" seen in vaginal secretions is positive for the presence of amniotic fluid due to ROM. 255

18-3. The TLi Analyzer, by Adeza Biomedical, is used to perform qualitative measurements of fetal fibronectin. 256

18-4. Immature epithelial cells (parabasal cells) as well as mature squamous epithelial cells. The immature cells are smaller and round. (Wet mount) 258

18-5. A predominance of parabasal cells in vaginal secretions is consistent with estrogen deficiency. In severely estrogen-deficient women, the vaginal fluid is almost acellular. (Wet mount) 258

18-6. Purulent vaginal secretion containing increased numbers of white blood cells, parabasal cells and absent lactobacilli are common findings in desquamative inflammatory vaginitis as well as other forms of vaginitis. (Wet mount) 258

18-7. Gram stain (1,000×). Lactobacillus predominating in a healthy vagina with squamous epithelial cells. (CDC, PHIL image, http://phil.cdc.gov/phil image 10g0029_lores.jpg.). 259

18-8. **A:** Wet mount and **(B)** Gram stain of "clue cells." These are squamous epithelial cells that are literally covered with numerous small curved bacilli. These cells slough off because of bacterial alteration in bacterial vaginosis. (From Sweet RL, Gibbs RS. *Atlas of Infectious Diseases of the Female Genital Tract*. Philadelphia, PA: Lippincott Williams & Wilkins; 2005, Asset 55832 c10f10.) 259

18-9. Trophozoites of *Trichomonas vaginalis* obtained from in vitro culture, stained with Giemsa. (CDC, DpDx Laboratory Diagnosis of Parasites of Public Health Concern Parasite Image Library, http://www.dpd.cdc.gov/dpdx/HTML/Image_Library.htm.). 260

18-10. Wet preparation of *Candida albicans* yeast and pseudohyphae with WBCs. Yeast (including pseudohyphae), RBCs, and WBCs (200×). (From McBride LJ. *Textbook of Urinalysis and Body Fluids: A Clinical Approach*. Philadelphia, PA: Lippincott; 1998.) 260

19-1. ICON pregnancy test cartridge. (Image courtesy of Beckman Coulter, Inc.) 264

19-2. Eosinophils in urine. Wright stain of cytocentrifuge preparation (400×). 264

19-3. This bronchoalveolar lavage is being performed with a protected catheter, but without the aid of a bronchoscope. (Image courtesy of.) 265

19-4. Normal bronchial epithelial cells in a bronchial brush specimen are shown. Note the ciliated columnar cells with uniform and basally located nuclei. The chromatin is finely granular and evenly dispersed, the nuclear membrane is smooth and regular, and the nucleoli are inconspicuous. (Papanicolaou stain) (Image courtesy of.) 265

19-5. Squamous cell carcinoma in a bronchial brush specimen. Highly atypical squamous cells show marked variation in size and shape. The nuclei are hyperchromatic and irregular. (Papanicolaou stain) (Image courtesy of.) 266

19-6. Adenocarcinoma cells in bronchial brush specimen. A cluster of epithelial cells with highly atypical nuclei, prominent nucleoli, and cytoplasmic vacuoles is seen. (Papanicolaou stain) (Image courtesy of.) 266

19-7. *Pneumocystis jiroveci* pneumonia. **A:** The alveoli are filled with a foamy exudate, and the interstitium is thickened and

© Jones & Bartlett Learning LLC, an Ascend Learning Company. NOT FOR SALE OR DISTRIBUTION.

contains a chronic inflammatory infiltrate (Hematoxylin & Eosin stain). **B:** A centrifuged bronchoalveolar lavage specimen impregnated with silver shows a cluster of Pneumocystis cysts. (Image courtesy of.) 266

19-8. Cytomegalovirus (CMV) infection in bronchial washings. Note the large basophilic nuclear inclusions surrounded by a halo and marginated chromatin, forming the typical target-shaped appearance. (Papanicolaou stain) (Image courtesy of.) 267

19-9. *Candida albicans* with germ tube development in a calcofluor white preparation. 267

19-10. Cell block preparation of BAL showing cysts of *P. jiroveci,* GMS-P stain (1,000×). (From McBride LJ. *Textbook of Urinalysis and Body Fluids: A Clinical Approach.* Philadelphia, PA: Lippincott; 1998:264.) 267

19-11. Cell block preparation of BAL showing cysts of *P. jiroveci,* GMS-P stain (1,000×). (From McBride LJ. *Textbook of Urinalysis and Body Fluids: A Clinical Approach.* Philadelphia, PA: Lippincott; 1998:265.) 267

19-12. Schematic of the middle ear. (Image courtesy of.) 267

19-13. Vitreous fluid is obtained by vitrectomy using simultaneous suction and infusion. **A:** Infusion of fluid through a 25-gauge needle secured by passing through a block of plastic sutured to the eye. **B:** Balanced salt solution is fed into the eye by gravity. **C:** Illumination and observation are provided with the indirect ophthalmoscope. **D:** The vitreous is aspirated into the port of the sharp-tipped vitreous cutter. (Image modified from.) 268

19-14. This image depicts histopathologic changes indicating aspergillosis of the lung caused by *Aspergillus fumigatus.* Methenamine silver stain reveals hyphae of *A. fumigatus.* Inhalation of airborne conidia of *A. fumigatus* can cause aspergillosis in immunosuppressed hosts. 269

19-15. Methenamine silver stain. Disseminated infection in an immune-compromised host with the opportunistic fungus, *A. fumigatus.* Note the characteristic dichotomous branching of the hyphae. 269

19-16. Bronchial washing cell block. H&E stain (1,000×). (From McBride LJ. *Textbook of Urinalysis and Body Fluids: A Clinical Approach.* Philadelphia, PA: Lippincott; 1998:263.) 269

19-17. Bronchial washing cell block. GMS-C stain (1,000×). (From McBride LJ. *Textbook of Urinalysis and Body Fluids: A Clinical Approach.* Philadelphia, PA: Lippincott; 1998:263.) 269

19-18. Bronchial washing cell block. PAP stain (1,000×). (From McBride LJ. *Textbook of Urinalysis and Body Fluids: A Clinical Approach.* Philadelphia, PA: Lippincott; 1998:263.) 269

20-1. Iris Automated Urinalysis iRICELL workcell. Product Images © 2009 IRIS International, Inc. All rights reserved. IRIS, the Iris logo, iChem, iQ, iRICELL, and Velocity are trademarks of IRIS International, Inc. and are registered in the USPTO.[AS7] 265

20-2. Iris Automated Urinalysis iRICELL workcell with iQ200ELITE. Product Images © 2009 IRIS International, Inc. All rights reserved. IRIS, the Iris logo, iChem, iQ, iRICELL, and Velocity are trademarks of IRIS International, Inc. and are registered in the USPTO. 265

20-3. Iris Automated Urinalysis iRICELL workcell with iQ200SELECT. Product Images © 2009 IRIS International, Inc. All rights reserved. IRIS, the Iris logo, iChem, iQ, iRICELL, and Velocity are trademarks of IRIS International, Inc. and are registered in the USPTO. 265

20-4. Iris Automated Urinalysis iRICELL workcell with iQ200SPRINT. Product Images © 2009 IRIS International, Inc. All rights reserved. IRIS, the Iris logo, iChem, iQ, iRICELL, and Velocity are trademarks of IRIS International, Inc. and are registered in the USPTO. 265

20-5. Close-up of the iQ barcode reader and tube carrier. 265

20-6. CLINITEK® Status. (Used with permission from Siemens Medical Solutions Diagnostics.) 265

20-7. CLINITEK Advantus® Analyzer. (Courtesy of Siemens Medical Solutions Diagnostics.) 265

20-8. CLINITEK Atlas® Automated Urine Chemistry Analyzer with rack. (Courtesy of Siemens Medical Solutions Diagnostics.) 265

20-9. CLINITEK Atlas® Automated Urine Chemistry Analyzer with carousel. (Courtesy of Siemens Medical Solutions Diagnostics.) 265

20-10. Fully Automated Urine Cell Analyzer UF-1000i. (Image courtesy of Sysmex America, Inc.) 265

20-11. Illustration of UF-1000i flow cytometry technology. (Image courtesy of Sysmex America, Inc.) 266

20-12. Digital images of urine sediment; white blood cells. 266

20-13. Digital images of urine sediment; red blood cells. 266

20-14. Digital images of urine sediment; transitional cells. 266

20-15. Digital images of urine sediment; hyaline casts. 266

20-16. Digital images of urine sediment; granular casts. 266

20-17. Digital images of urine sediment; calcium oxalate crystals. 266

20-18. Digital images of urine sediment; triple phosphate crystals. 266

20-19. Digital images of urine sediment; bacteria. 266

20-20. Digital images of urine sediment; these sperm were classified by the instrument at bacteria and must be reassigned to the correct category. Not all facilities report sperm in urine sediment. 266

20-21. Digital images of urine sediment; yeast. 266

20-22. Squamous epithelial cells are not usually reported and are identified as "unclassified" urinary sediment. 266

20-23. Compilation of urine sediment digital images; artifacts. **A:** Air bubble. **B:** Amorphous material/crystals. **C:** Mucous strands may be mistaken for casts, especially if they have debris or cells attached as seen in the one on the left. 266

20-24. Iris iQ Body Fluid Module. Product Images © 2009 IRIS International, Inc. All rights reserved. 266

20-25. The Sysmex Hematology-XN-100 includes a body fluid mode. (Image courtesy of Sysmex America, Inc.) 267

20-26. SQA-V *Gold* Sperm analyzer. (Image courtesy of Medical Electronic Systems.) 267

20-27. QwikCheck *Gold* Sperm analyzer. (Image courtesy of Medical Electronic Systems.) (Not currently available for the U.S. market.) 267

20-28. SQAIIC-P Sperm analyzer. (Image courtesy of Medical Electronic Systems.) (Not currently available for the U.S. market.) 267

20-29. CLINITEST hCG test for use with the CLINITEK Status family of analyzers. (Courtesy of Siemens Medical Solutions Diagnostics.). 267

20-30. Polymedco OC-Auto 80 FOBT analyzer; external view. 267

20-31. Polymedco FOBT sample collection vial/bottle. 267

20-32. Polymedco OC-Auto 80 FOBT analyzer; internal view. 267

© Jones & Bartlett Learning LLC, an Ascend Learning Company. NOT FOR SALE OR DISTRIBUTION.

List of Tables

Chapter 2

Table 2-1 Characteristics of Nephritic and Nephrotic Syndromes 22
Table 2-2 RIFLE Criteria for Acute Kidney Injury (Developed by a Panel of the Acute Dialysis Initiative Group) 27
Table 2-3 Urinalysis Casts and Renal Disease 27
Table 2-4 Laboratory Findings in Urinary and Kidney Diseases 28

Chapter 3

Table 3-1 Porphyrin and Porphyrin Precursors in the Urine 39

Chapter 4

Table 4-1 Examples of Laboratory Testing Errors 47
Table 4-2 Classes of Fire Extinguishers and Their Uses 49

Chapter 6

Table 6-1 Changes Occurring to Unpreserved Urine 76

Chapter 7

Table 7-1 Causes for Urine Color and Clarity 81

Chapter 8

Table 8-1 Protein Indicators and Sensitivities by Reagent Strip 92
Table 8-2 Glucose Chromogens and Sensitivities by Reagent Strip 95
Table 8-3 Interpretation of Glucose Oxidase and Copper Reduction Tests 96
Table 8-4 Ketone Reagents and Sensitivities by Reagent Strip 97
Table 8-5 Hemoglobin Chromogens and Sensitivities by agent Strip 99
Table 8-6 Bilirubin Indicators and Sensitivities by Reagent Strip 102
Table 8-7 Urobilinogen Reagents and Sensitivities by Reagent Strip 104
Table 8-8 Nitrite Reagents and Sensitivities by Reagent Strip 105
Table 8-9 Leukocyte Esterase Reagents and Sensitivities by Reagent Strip 106

Chapter 9

Table 9-1 Properties of Crystalline Compounds 119

Chapter 11

Table 11-1 Commonly Analyzed Body Fluids 180
Table 11-2 Commonly Used Terms in the Description of Body Fluid Appearance 180

Chapter 12

Table 12-1 Causes for Pleocytosis in Cerebrospinal Fluid (CSF) by Cell Type 189
Table 12-2 Changes in Cells Present in Cerebrospinal Fluid (CSF) Following Hemorrhage 191

Chapter 13

Table 13-1 Bacteria Commonly Seen in Effusions 203
Table 13-2 Differentiation Between Transudates and Exudates 204
Table 13-3 Laboratory Differentiation of Chylous and Pseudochylous Effusions 205
Table 13-4 Causes for Various Body Cavity Effusions 206

Chapter 14

Table 14-1 Mucin Clot Procedure According to Referenced Texts 214
Table 14-2 Classification of Synovial Fluids 218

Chapter 16

Table 16-1 Semen Classifications 234
Table 16-2 Normal Semen Analysis Ranges 234
Table 16-3 Semen Biochemical Markers 242

Chapter 18

Table 18-1 Toxicity of Swabs to Microorganisms 255

Chapter 20

Table 20-1 Automated Urinalysis Instruments 264
Table 20-2 Automated Body Fluid Analyzers 266

© Jones & Bartlett Learning LLC, an Ascend Learning Company. NOT FOR SALE OR DISTRIBUTION.

© Jones & Bartlett Learning LLC, an Ascend Learning Company. NOT FOR SALE OR DISTRIBUTION.

Contents

Contributor vii
Reviewers vii
Preface ix
Content Highlights xi
About the Authors xiii
Acknowledgments xv
List of Figures xvii
List of Tables xxix

SECTION I Foundational Information

CHAPTER 1 Urinary System Anatomy and Physiology and Urine Formation 2

CHAPTER 2 Renal and Urinary Tract Diseases and Related Urinalysis Findings 18

CHAPTER 3 Metabolic Diseases and Related Urinalysis Findings 34

CHAPTER 4 Urinalysis Clinical Laboratory Operations 44

CHAPTER 5 Microscopy 55

SECTION II The Urinalysis

CHAPTER 6 Collection and Preservation of Urine 72

CHAPTER 7 Physical Examination of Urine 79

CHAPTER 8 Chemical Analysis of Urine 89

CHAPTER 9 Microscopic Examination of Urinary Sediment 111

CHAPTER 10 Atlas of Urinary Sediment 142

© Jones & Bartlett Learning LLC, an Ascend Learning Company. NOT FOR SALE OR DISTRIBUTION.

SECTION III Body Fluids Analysis

CHAPTER 11 Introduction to Body Fluids 178

CHAPTER 12 Cerebrospinal Fluid 184

CHAPTER 13 Serous Body Fluids 199

CHAPTER 14 Synovial Fluid 211

CHAPTER 15 Gastric Fluid and Fecal Analysis 221

CHAPTER 16 Semen Analysis 231

CHAPTER 17 Amniotic Fluid 246

CHAPTER 18 Vaginal Secretions 254

CHAPTER 19 Miscellaneous Urine and Body Fluid Tests 263

CHAPTER 20 Automation of Urinalysis and Body Fluids Examination 271

APPENDICIES

Appendix A Answers to Study Guide Questions and Case Studies 281

Appendix B Reagent Strip Color Chart 289

Appendix C Hemocytometer Cell Counts 291

Appendix D Historically Relevant Urine and Body Fluid Analysis Information 295

Glossary 303
Index 313

© Jones & Bartlett Learning LLC, an Ascend Learning Company. NOT FOR SALE OR DISTRIBUTION.